Molecular Phylogenetics and Evolution 125 (2018) 100–115

Contents lists available at ScienceDirect

Molecular Phylogenetics and Evolution

journal homepage: www.elsevier.com/locate/ympev

# Resolving complex phylogeographic patterns in the Balkan Peninsula using closely related wall-lizard species as a model system

Nikolaos Psonis[a,b,*], Aglaia Antoniou[c], Emmanouela Karameta[d], Adam D. Leaché[e], Panayiota Kotsakiozi[f], Diego Darriba[g], Alexey Kozlov[g], Alexandros Stamatakis[g,h], Dimitris Poursanidis[i], Oleg Kukushkin[j,k], Daniel Jablonski[l], Jelka Crnobrnja–Isailović[m,n], Iulian Gherghel[o,p], Petros Lymberakis[a], Nikos Poulakakis[a,b]

[a] Natural History Museum of Crete, School of Sciences and Engineering, University of Crete, Knosos Avenue, Irakleio GR71409, Greece
[b] Department of Biology, School of Sciences and Engineering, University of Crete, Vassilika Vouton, Irakleio GR70013, Greece
[c] Institute of Marine Biology, Biotechnology and Aquaculture, Hellenic Centre for Marine Research, Gournes Pediados, P.O. Box 2214, Irakleio GR71003, Greece
[d] Section of Zoology and Marine Biology, Department of Biology, National and Kapodistrian University of Athens, Panepistimioupolis, Athens 157-84, Greece
[e] Department of Biology and Burke Museum of Natural History and Culture, University of Washington, Seattle, WA, USA
[f] Department of Ecology and Evolutionary Biology, Yale University, 21 Sachem Street, New Haven, CT 06520-8105, USA
[g] The Exelixis Lab, Scientific Computing Group, Heidelberg Institute for Theoretical Studies, Schloss-Wolfsbrunnenweg 35, 69118 Heidelberg, Germany
[h] Karlsruhe Institute of Technology, Institute for Theoretical Informatics, Postfach 6980, 76128 Karlsruhe, Germany
[i] Foundation for Research and Technology – Hellas (FORTH), Institute of Applied and Computational Mathematics, N. Plastira 100, Vassilika Vouton, Iraklion GR70013, Greece
[j] Department of Biodiversity Studies and Ecological Monitoring, T.I. Vyazemski Karadag Research Station – Nature Reserve of Russian Academy of Sciences, Nauki Str. 24, stm. Kurortnoe, Theodosia 298188, Republic of the Crimea, Russia
[k] Department of Herpetology, Institute of Zoology of Russian Academy of Sciences, Universitetskaya Emb. 1, Saint Petersburg 199034, Russia
[l] Department of Zoology, Comenius University in Bratislava, Mlynská dolina, Ilkovičova 6, 842 15 Bratislava, Slovakia
[m] Department of Biology and Ecology, Faculty of Sciences and Mathematics, University of Niš, Višegradska 33, Niš 18000, Serbia
[n] Department of Evolutionary Biology, Institute for Biological Research "Siniša Stanković", University of Belgrade, Despota Stefana 142, Beograd 11000, Serbia
[o] Department of Biology, Case Western Reserve University, 2080 Adelbert Road, Cleveland, OH 44106, USA
[p] Faculty of Geography and Geology, Alexandru Ioan Cuza University of Iasi, Carol I Bvd, no 20A, Iasi, Romania

ARTICLE INFO

*Keywords:*
ddRADseq
MessinianSalinity Crisis
Quaternary climatic refugia
Phylogenomics
*Podarcis tauricus* species subgroup
Population structure

ABSTRACT

The Balkan Peninsula constitutes a biodiversity hotspot with high levels of species richness and endemism. The complex geological history of the Balkans in conjunction with the climate evolution are hypothesized as the main drivers generating this biodiversity. We investigated the phylogeography, historical demography, and population structure of closely related wall-lizard species from the Balkan Peninsula and southeastern Europe to better understand diversification processes of species with limited dispersal ability, from Late Miocene to the Holocene. We used several analytical methods integrating genome-wide SNPs (ddRADseq), microsatellites, mitochondrial and nuclear DNA data, as well as species distribution modelling. Phylogenomic analysis resulted in a completely resolved species level phylogeny, population level analyses confirmed the existence of at least two cryptic evolutionary lineages and extensive within species genetic structuring. Divergence time estimations indicated that the Messinian Salinity Crisis played a key role in shaping patterns of species divergence, whereas intraspecific genetic structuring was mainly driven by Pliocene tectonic events and Quaternary climatic oscillations. The present work highlights the effectiveness of utilizing multiple methods and data types coupled with extensive geographic sampling to uncover the evolutionary processes that shaped the species over space and time.

## 1. Introduction

Located at the crossroads of three continents, the Mediterranean Basin combines different cultural, geological and biological features of Europe, Asia and Africa, and represents one of the richest and most complex regions on Earth (Blondel et al., 2010). Species richness and genetic diversity are notably higher in the southern European peninsulas extending into the Mediterranean Sea (Iberian, Italian, and the

* Corresponding author at: Department of Biology, School of Sciences and Engineering, University of Crete, Vassilika Vouton, Irakleio GR70013, Greece.
*E-mail address:* nikos.psonis@gmail.com (N. Psonis).

https://doi.org/10.1016/j.ympev.2018.03.021
Received 17 July 2017; Received in revised form 8 March 2018; Accepted 14 March 2018
Available online 21 March 2018
1055-7903/ 

Balkans), compared to higher latitudes (Hewitt, 2011), rendering them as biodiversity hotspots (Blondel and Aronson, 1999; Myers et al., 2000). The Balkan peninsula has played a key role as a source of postglacial colonization of central and northern Europe (Griffiths et al., 2004) and generally hosts higher species richness in comparison to the Iberian and the Italian ones, yet still remains phylogeographically understudied (Hewitt, 2011). This comes as no surprise considering the complex geological history of this area. The Eocene orogeny was followed by successive connections or land mass submergence, that were more pronounced in the Miocene and the Pliocene (22–2.56 Mya), e.g. the progressive fragmentation of the Aegean landmass (comprising the Balkans and western Turkey) by the formation of the Mid Aegean Trench (MAT) (Creutzburg, 1963; Dermitzakis and Papanikolaou, 1981). These events provided many opportunities for dispersal and vicariance throughout this period and might be responsible for the high species diversity observed today. Indeed, phylogeographic studies on various taxa of this region have revealed extensive intra- and interspecific divergence in this period (Poulakakis et al., 2014).

The southwestern part of the Balkans, defined by the Dinarides and External Hellenides of continental Greece and southern Albania mountain ranges (Pindos Mts., Fig. 1A) and their adjacent areas, represent one of the richest areas of Europe in reptile species (Džukić and Kalezić, 2004; Sillero et al., 2014). These mountain ranges have acted as important biogeographic barriers for numerous species (Lymberakis and Poulakakis, 2010) including lizards (Gvoždík et al., 2010; Marzahn et al., 2016; Sagonas et al., 2014; Valakos et al., 2008), snakes (Ferchaud et al., 2012; Guicking et al., 2009; Mizsei et al., 2017; Musilová et al., 2010; Ursenbacher et al., 2008), frogs (Džukić and Kalezić, 2004; Valakos et al., 2008)], insects (Allegrucci et al., 2009)], spiders (Kornilios et al., 2016)], and land snails (Kotsakiozi et al., 2012; Psonis et al., 2015; Welter-Schultes, 2012). Furthermore, the aforementioned mountain ranges have also affected the fauna of the Peloponnese (Fig. 1A) as indicated by the fact that several closely related taxa (see above studies) are only distributed in the western part of Pindos Mts. and in the Peloponnese. This fact, in conjunction with the complex geological history of the Peloponnese (Creutzburg, 1963) and the climatic changes since the Tertiary (Zachos et al., 2001), has given rise to a plethora of Peloponnesian endemic species that exhibit high levels of genetic diversity [e.g. *Algyroides moreoticus, Hellenolacerta graeca*, *P. peloponnesiacus*, and *Anguis cephallonica* (Valakos et al., 2008)].

During the Pleistocene, glacial refugia were highly important for the maintenance and promotion of biodiversity, especially for the species (endemics or not) that shifted their ranges (Barbosa et al., 2017). Therefore, numerous phylogeographic studies have focused on the expansion of widespread temperate species from 'glacial refugia' (Hewitt, 2000 and references therein). However, geographic, habitat and climatic heterogeneity within the glacial refugia may have often subdivided populations resulting in 'refugia within refugia' (Abellán and Svenning, 2014; Gomez and Lunt, 2007). Describing the genetic patterns within refugia is paramount to the interpretation of the structure of both widespread species that have expanded their ranges far beyond the refugia, and species that are currently restricted therein, i.e., 'refugial endemics' (Bilton et al., 1998; Kryštufek et al., 2007).

The wall lizards of the genus *Podarcis* have been assigned to several species groups (Harris and Arnold, 1999; Oliverio et al., 2000) with the focal taxa of this study falling into the Balkan species group and the *Podarcis tauricus* species subgroup (Poulakakis et al., 2005a, 2005b; Psonis et al., 2017). The species subgroup includes at least five species that inhabit southeastern Europe. These include *P. gaigeae* (Werner, 1930) and *P. milensis* (Werner, 1930), which are Aegean endemics of the Skyros and Milos island groups, respectively, *P. melisellensis* (Braun, 1877) along the Dalmatian coasts, with high intraspecific genetic differentiation (Podnar et al., 2004), and two putative species within *P. tauricus* species complex, hereafter named *P. ionicus* (exhibiting high genetic diversification with five distinct subclades *a-e*) and *P. tauricus*, as proposed by Psonis et al. (2017). The two latter putative species have evolved allopatrically in the western and the eastern parts of the

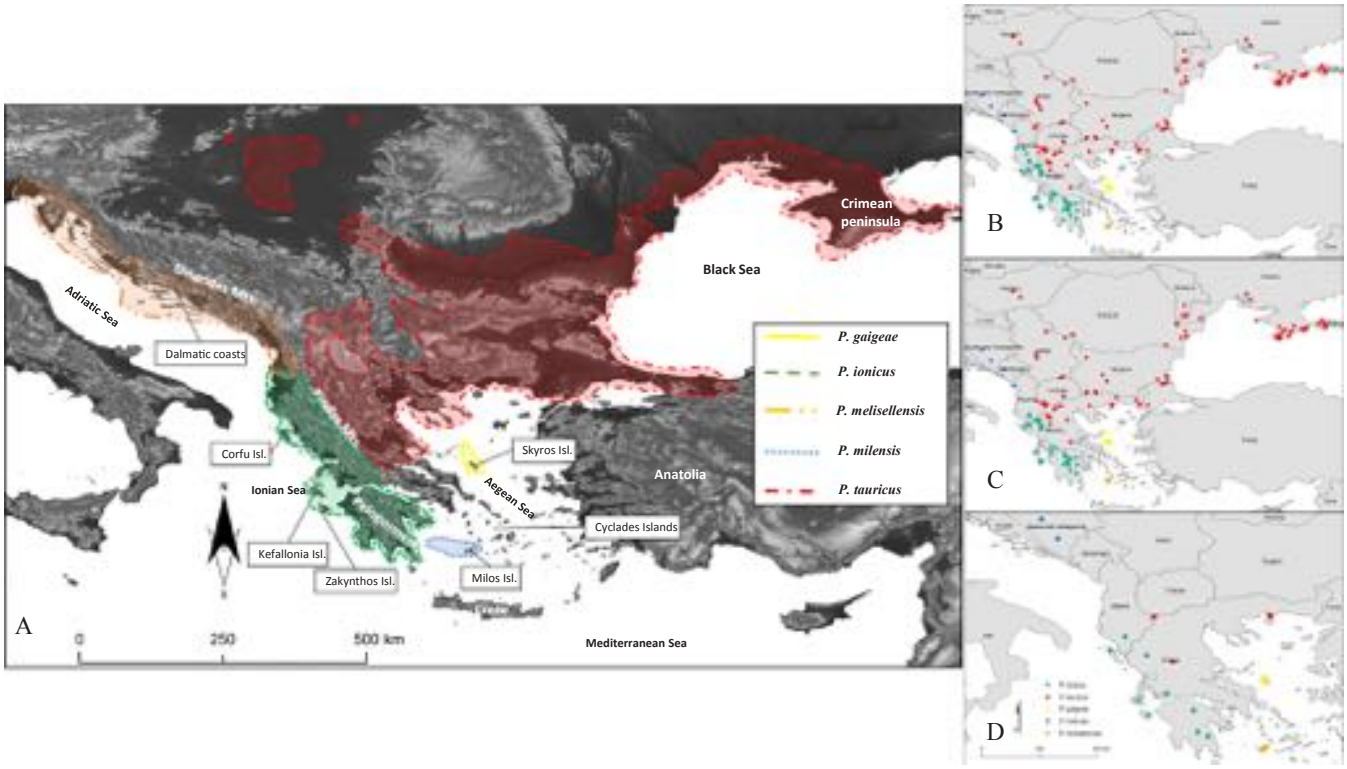


**Fig. 1.** (A) Species distribution of *Podarcis tauricus* species subgroup in Southern Europe according to IUCN. (B) The geographic localities of all specimens used in the present study). (C) and (D) indicate the geographic localities of the specimens used in the analyses with microsatellites data and phylogenomic analyses with ddRADseq data. Multiple samples may have been collected in some sites.

**Table 1**
Species and subspecies of the *Podarcis tauricus* species subgroup according to the literature, clades/subclades identified by Podnar et al. (2004) and Psonis et al. (2017), the classification system followed in the present study based on suggestions of the these studies, and the taxa/clades distribution.

| Recognized species | Recognized subspecies | Identified clades/ subclades | Classification system followed in the present study | Distribution |
|---|---|---|---|---|
| *Podarcis gaigeae* | *P. g. gaigeae* | *P. gaigeae* | *P. gaigeae* (no subspecies) | Skyros Isl. and satellite islets, Greece |
| | *P. g. weigandi* | | | Piperi islet (Northern Sporades Islands), Greece |
| *Podarcis melisellensis* | *P. m. melisellensis* | *P. m. melisellensis* | *P. m. melisellensis* (Samples not included) | Jabuka Isl., Brusnik Isl., Biševo Isl. and Vis Isl. and satellite islets, Croatia |
| | *P. m. fiumanus* | *P. m. fiumanus* | *P. m. fiumanus* | Italy (near Trieste), Croatian coast including many offshore islands and islets, Bosnia-Herzegovina, Montenegro and northwestern Albania |
| | *P. m.* ssp. (Lastovo) | Lastovo subclade | Lastovo subclade (Samples not included) | Lastovo Isl. and satellite islets, Croatia |
| *Podarcis milensis* | *P. m. milensis* | *P. m. milensis* | *P. m. milensis* | Milos Isl., Kimolos Isl., Polyaigos Isl. and Antimilos Isl. and their satellite islets, Greece |
| | *P. m. gerakuniae*[*] | Not included in the studies | *P. m. gerakuniae* (Samples not included) | Falkonera islet and Velopoula islet, (W of Milos Isl.), Greece |
| | *P. m. adolfjordansi*[*] | Not included in the studies | *P. m. adolfjordansi* (Samples not included) | Ananes islet (SW of Milos Isl.), Greece |
| *Podarcis tauricus* | *P. t. tauricus* | *P. tauricus* | *P. tauricus* (no subspecies) | From Crimean peninsula and southern Ukraine, through southern Moldova, and eastern and southern Romania (excluding the Danube Delta), to Bulgaria, F.Y.R.O.M., eastern and southern Serbia, Albania, mainland Greece (east side of Pindos Mt. excluding central Greece and Evvoia Isl.), northwestern Turkey, and Hungary. |
| | *P. t. thasopulae* | | | Thasopoula islet (N of Thasos Isl.), Greece |
| | *P. t. ionicus* | Subclade *a* | *P. ionicus* subclade *a* | Ithaca Isl., Kefallonia Isl., Zakynthos Isl, Strofades islets (south of Zakynthos Isl.), Greece |
| | | Subclade *b* | *P. ionicus* subclade *b* | Southwestern central Greece |
| | | Subclade *c* | *P. ionicus* subclade *c* | Northeastern Peloponnese, Greece |
| | | Subclade *d* | *P. ionicus* subclade *d* | Central and southeastern Peloponnese, Greece |
| | | Subclade *e* | *P. ionicus* subclade *e* | West Peloponnese and northwestern mainland Greece including Corfu Isl. and southwestern Albania |

[*] *P. m. gerakuniae* and *P. m. adolfjordansi* have never been analyzed genetically.

External Hellenides (Pindos Mts.), respectively (Fig. 1A and Table 1). A thorough understanding of the evolutionary and adaptive history of the *P. tauricus* species subgroup has been hampered by the lack of genome-wide data, as traditional mitochondrial (mtDNA) and nuclear (nDNA) markers have failed to resolve key phylogenetic relationships within this subgroup (Psonis et al., 2017 and references therein). The main issue is the existence of polytomies both among and within the five species of the subgroup. These polytomies were attributed to rapid diversification (Psonis et al., 2017), a phenomenon quite common in Lacertidae (Pavlicev and Mayer, 2009) and especially in *Podarcis* (Oliverio et al., 2000), rendering the use of numerous and more appropriate molecular markers indispensable (Psonis et al., 2017).

Double-digest Restriction site associated DNA sequencing (ddRADseq) is emerging as one of the most useful reduced-representation genome sequencing methods for phylogenetic and population-level studies (Peterson et al., 2012), providing thousands of SNPs suitable for estimating high-resolution phylogenetic trees (DaCosta and Sorenson, 2016; Leaché et al., 2015; Nieto-Montes de Oca et al., 2017). These genome-wide approaches coupled with Species Distribution Modelling (SDM) methods may provide deeper insights into the historical biogeography of the species subgroup (Blois, 2012; Psonis et al., 2016; Senczuk et al., 2017; Svenning et al., 2011; Wielstra et al., 2013) and can also be used to test niche similarity and overlap between extant species and niche evolution across phylogenies (Ahmadzadeh et al., 2016, 2013; Rato et al., 2015).

The main scope of the present study is to improve our understanding of the processes that produced the high genetic and species diversity found in the Balkan Peninsula, using the *P. tauricus* species subgroup as a case study, as it is distributed along the entire focal area with high levels of genetic diversity (Psonis et al., 2017). In order to address these questione, we employed a multi-level approach, studying the evolutionary history of the entire subgroup, considering processes that impacted multiple taxonomic levels from populations to species, using a sampling scheme that covers the distribution of the subgroup and estimated its diversification over time from the Late Miocene to the Holocene. To improve our inferences we used multiple analytical methods incorporating genome-wide SNPs (ddRADseq), nuclear (nDNA) and mitochondrial (mtDNA) DNA sequences, as well as microsatellites. We used these methods and data to investigate (a) phylogenomic relationships, (b) phylogeography, (c) population structure, (d) historical demography, and (e) contemporary distribution and niche overlap of all taxa and populations belonging to the focal species subgroup.

## 2. Material and methods

Overall, we used a total of 420 specimens of the *P. tauricus* species subgroup was used in our analyses, including 65 specimens of *P. gaigeae*, 86 of *P. ionicus*, 10 of *P. melisellensis*, 58 of *P. milensis*, and 201 of *P. tauricus* (Fig. 1B and Table S1). However, not the same individuals were analyzed at all genetic markers (see below). Total genomic DNA was extracted from muscle tissue or blood using a typical ammonium acetate protocol (Bruford et al., 1998) or the DNeasy Blood & Tissue Extraction kit (Qiagen®, Hilden, Germany). DNA quality and quantity was evaluated using agarose gel electrophoresis (TAE 1.5%) and the Qubit® 2.0 Fluorometer (Invitrogen®, Carlsbad, California, USA), respectively.

### 2.1. Phylogenomics (ddRADseq) on Podarcis tauricus species subgroup

#### 2.1.1. ddRADseq - Taxon sampling

We collected genome-wide SNPs via the ddRADseq method from 36 specimens (Fig. 1D) representing each major clade and subclade of the *P. tauricus* species subgroup, (Podnar et al., 2004; Poulakakis et al., 2005a, 2005b; Psonis et al., 2017). In particular, we included five specimens of *P. gaigeae*, 11 of *P. ionicus*, two of *P. melisellensis*, six of *P. milensis*, and 12 of *P. tauricus* (Table S1). We also included 10 specimens from five closely related species as outgroups (two each for *P. cretensis*, *P. erhardii, P. levendis*, *P. muralis,* and *P. peloponnesiacus*).

#### 2.1.2. ddRADseq - Data collection

The ddRADseq library was prepared using 500 ng of genomic DNA and two restriction enzymes (SbfI and MspI; New England Biolabs) based on the protocol described by Peterson et al. (2012). The sequencing of the library was performed on an Illumina HiSeq 2000 lane (Illumina Inc., San Diego, California, USA) (100-bp, single end reads) at the QB3 facility at the University of California, Berkeley (California, USA). The detailed procedure followed can be found in the Supporting Text S1. Raw Illumina reads were processed with pyRAD (v3.0.6; Eaton, 2014) using three different clustering threshold values (Wclust equal to 0.85, 0.90, and 0.95), as this parameter has been shown to affect phylogenetic relationships (Leaché et al., 2015). To assess the impact of missing data on phylogenetic inference and to determine the minimum amount of data that carry sufficient phylogenetic signal for resolving the topology, we constructed a set of supermatrices by selecting subsets of loci according to the minimum number of unique sequences per locus (min_taxa). The subsets were selected such that they most closely contain 100% (min_taxa = 4), 50% (min_taxa = 7), 25% (min_taxa = 9), and 12.5% (min_taxa = 11) of the loci, respectively. Overall, 12 datasets were assembled (three clustering thresholds × four min_taxa filters). Details on the bioinformatics pipeline followed for ddRADseq data filtering and dataset generation are presented in the Supporting Text S2.

#### 2.1.3. ddRADseq - Phylogenomic analyses (concatenated loci tree)

To evaluate the stability of the phylogenetic signal for each assempled dataset we first performed a Maximum Likelihood tree inference using ExaML (v.3.0.17; Kozlov et al., 2015) with 100 random starting trees (random seed numbers). Then, we used the 100 resulting topologies to calculate the average Robinson Foulds distance (RF distance; Robinson and Foulds, 1981) in each of the 12 datasets. Based on these distances, we selected the most stable dataset for further analyses. Using the selected dataset, we calculated bootstrap values in RAxML (v.8.2.9; Stamatakis, 2014). Bootstrap support was reported onto the best-scoring tree of the selected dataset. We also constructed a Bayesian Inference tree in ExaBayes (v.1.5; Aberer et al., 2014). Details on the evaluation of the phylogenetic signal and on the Maximum Likelihood and Bayesian Inference phylogenetic analyses using the selected concatenated dataset are given in the Supporting Text S3.

#### 2.1.4. ddRADseq - Phylogenomic analyses (species tree)

To fully exploit the power of the ddRADseq data (i.e., both sequences and genotypes), we obtained a SNP based species tree using the multispecies coalescent method SVDQuartets (Chifman and Kubatko, 2014) as implemented in PAUP (v.4.0a152; Swofford, 2002). This method infers the topology among randomly sampled quartets of predefined species, and then a quartet method is used to assemble the sampled quartets into a species tree. An exhaustive search of quartet sampling was selected and the uncertainty in relationships was measured using non-parametric bootstrapping with 100 replicates.

#### 2.1.5. ddRADseq - Reconstruction of the ancestral geographical distribution

We used a combination of phylogenetic and distributional information to infer the genus evolution in southeastern Europe. The ancestral area reconstruction method employed was the Dispersal-Extinction-Cladogenesis analysis (DEC) implemented in LAGRANGE (Ree and Smith, 2008) using the Reconstruct Ancestral States in Phylogenies (RASP; Yu et al., 2013) software. For this biogeographic analysis we used the ddRADseq phylogenomic tree from the BI analysis. We assigned all taxa (species/subspecies/populations) to eight geographic areas: (i) northwestern Balkans (including all specimens of *P. melisellensis*), (ii) eastern Balkans and Southern Europe (i.e, Moldavia, Ukraine, and Crimean peninsula) including all specimens of *P. tauricus*,

(iii) Skyros Island group (including all specimens of *P. gaigeae*), (iv) Milos Island group (including all specimens of *P. milensis*), (v) the Peloponnese (including all specimens of *P. ionicus* distributed in the area), (vi) south Ionian islands (including all specimens of *P. ionicus* distributed on Kefalonia and Zakynthos Islands), (vii) west central continental Greece (including all specimens of *P. ionicus* distributed in the area around the lake Trichonida), and finally (viii) northwestern continental Greece and southwestern Albania [including all specimens of *P. ionicus* distributed in this range, including on the Ionian island of Corfu (Kerkyra), as this island was isolated from the mainland during the Holocene (Perissoratis and Conispoliatis, 2003)]. The geographic locations mentioned can be found on the maps of Fig. 1A and S10.

#### 2.1.6. ddRADseq – SNPs based population structure analysis

We inferres population structure using the Bayesian clustering method implemented in STRUCTURE (v.2.3.4, Pritchard et al., 2000) and the dataset of Wclust = 0.85. The correlated allele frequency with admixture model (F-model) was applied. Given the number of *K* clusters, this model pursues solutions that are, as far as possible, in Hardy-Weinberg and linkage equilibrium. In this study, five replicate runs were performed for each *K* that ranged from 1 to 10. Each run comprised 200,000 generation as burn-in period, followed by 800,000 MCMC iterations from which the results were collected. Using longer MCMC runs did not modify the results. The inference of *K* was evaluated by the ΔK method (Evanno et al., 2005) using the software STRUCTURE HARVESTER (Earl and vonHoldt, 2012). The program CLUMPP v1.1.2 (Jakobsson and Rosenberg, 2007) was used to define run modes (if more than one), to generate consensus solutions allowing for label switching, to test for convergence from the five independent STRUCTURE runs, and to provide the Q values based on which a population or an individual can be assigned to a specific cluster above a given value (here Q = 0.90). The results were plotted using DISTRUCT v.1.1 (Rosenberg, 2004). To complement this analysis we used a multivariate approach that does not seek to maximize HW equilibrium as the previous one. We used Discriminant Analysis of Principal Components (DAPC) (Jombart et al., 2010) implemented in the R package adegenet (v.1.3.1, Jombart and Ahmed, 2011). We assumed nine predefined populations corresponding to the nine major clades and subclades of the *P. tauricus* species subgroup suggested by Psonis et al. (2017). To prevent overfitting of the DAPC, the number (five) of retained principal components (PCs) was chosen according to the optimal *α*-score.

### 2.2. Microsatellites data - Population genetics on Podarcis tauricus species subgroup

Since the cost of NGS methods prevents the analysis of large numbers of individuals, we also screened a subset of the 420 individuals for microsatellites loci variation to complement to SNPs based analyses (e.g. Antoniou et al., 2017).

#### 2.2.1. Microsatellites data – Taxon sampling and genotyping

Seventeen microsatellite loci designed/developed for the genera of *Podarcis* and *Lacerta* were amplified in multiplex PCRs (see Table S2). The microsatellite dataset consisted of 60 specimens of *P. gaigeae*, 10 of *P. melisellensis*, 56 of *P. milensis*, 197 of *P. tauricus*, and 84 of *P. ionicus* (Fig. 1**C**). Table S1 shows the individuals analyzed and if they were scored at other markers.

PCR products were combined in five multi-loading schemes (Table S2) and genotyped on an ABI 3730 (Applied Biosystems) using GS-500 Liz (Applied Biosystems) as an internal size standard in each capillary. Genotypes were determined using the STRand software (v.2.4.0.59, Toonen and Hughes, 2001) (http://www.vgl.ucdavis.edu/STRand). To minimize the negative consequences of poor allele calling, binning was accomplished with Flexibin 2 (v.2, Amos et al., 2007) the output of which was manually evaluated.

#### 2.2.2. Microsatellites data – Summary statistics

The software MICRO-CHECKER (v.2.2.3, van Oosterhout et al., 2004) was used to check for per-locus heterozygote deficit, the presence of null alleles, large allele dropout, and possible scoring errors. GENEPOP (v.3.4, Raymond and Rousset, 1995) was used to estimate measures of genetic diversity [number of alleles per locus (*A*), $F_{IS}$ index (Weir and Cockerham, 1984), expected (H*e*) and observed (H*o*) heterozygosity per locus] and to test for Hardy–Weinberg (HW) equilibrium. The above parameters were estimated in several different datasets, including the entire dataset (all samples) and clusters revealed by the population STRUCTURE analyses (nine sub-datasets; see below). We used GENETIX (Belkhir et al., 2001) to estimate pairwise F*st* values (Weir and Cockerham, 1984) with statistical significance evaluated over 1000 permutations.

Following Gariboldi et al. (2016), we used ML-RELATE (Kalinowski et al., 2006) to identify potential parent–offspring and full sibling pairs, as relatedness could impact downstream results interpretation. After determining the most likely pairwise relationship (first order, second order, or unrelated) within each species, we performed the relatedness specific hypothesis test with $1 \times 10^5$ simulations of random genotype pairs in order to determine whether the putative relationship (parent–offspring or full sibling) has a better fit to the data compared to the alternative relationship (full sibling or half sibling, respectively) (p-value = 0.001).

#### 2.2.3. Microsatellites data – Population structure

The underlying population structure based on microsatellites was inferred by methods implemented in STRUCTURE and DAPC (50 PCs) as described in Section 2.1.6. We used hierarchical STRUCTURE analysis (Vähä et al., 2007) to recursively infer clustering patterns in each major cluster, as suggested by Evanno et al. (2005). Each reiteration was carried out using only individuals with high membership value to a given cluster (here Q ≥ 0.90).

#### 2.2.4. Microsatellites data – Historical demographic inference and recent migration detection

Since the SNP dataset, given its small number of individuals and populations, could not be used to detect signatures of demographic events, we carried out historical demographic analyses using the microsatellites dataset on each of the nine clusters revealed by the hierarchical STRUCTURE analysis.

To evaluate demographic size changes we used BOTTLENECK (v.1.2.02; Cornuet and Luikart, 1996; Piry et al., 1999) under a two-phase model (TPM) constraining the model by defining 90% of mutations as conforming to a stepwise mutation model and 10% as multistep. We also carried out two demographic expansion tests, the k intralocus variability statistic (or kurtosis test; k-test) and the g interlocus variability statistic (g-test) as described by Reich et al. (1999), using the macro program kgtests (Bilgin, 2007) implemented in Microsoft Excel ®.

Recent migration rate (*m*) among the nine clusters identified by the hierarchical structuring analysis was estimated using BayesAss (v. 3.0.4; Wilson and Rannala, 2003). The program uses genotypes to estimate rates of recent migration among populations, without requiring HWE within populations (Wilson and Rannala, 2003). Two independent runs of $5 \times 10^7$ generations (sampling every 2000) with $3 \times 10^7$ generations omitted as burn-in were performed. After performing initial test runs we used the proposed step size for the different parameters (delta values) was adjusted to: $m = 0.2$, $a = 0.4$, and $f = 0.2$, as more reliable results are obtained when the acceptance rates of proposed changes for allele frequencies (*a*), inbreeding coefficient (*f*), and migration rate (*m*) are between 40 and 60% of the total chain length (http://rannala.org/docs/BayesAss.1.3.pdf).

### 2.3. Sanger sequencing data

#### 2.3.1. Mitochondrial DNA data - Historical demographic inference

To complement and compare the results of the previous analyses we also performed historical demographic analyses [mismatch distributions, Bayesian Skyline Plots (BSP), and haplotype networks] and estimated demographic and diversity indices using previously published mtDNA data (Podnar et al., 2004; Poulakakis et al., 2005a, 2005b; Psonis et al., 2017). In total, 324 sequences (298 of them belonging to the same specimens as those used in microsatellites analyses) were used, including 18 of *P. gaigeae*, 15 of *P. melisellensis*, 30 of *P. milensis*, 175 of *P. tauricus* and 86 of *P. ionicus* (see Table S1 for sample information) for each main clade and subclade identified in Psonis et al. (2017). More details about mtDNA analyses can be found in the Supporting Text S4).

#### 2.3.2. Mitochondrial and nuclear DNA data – Estimation of divergence times within the Podarcis tauricus species subgroup

To estimate divergence times among the major clades of the *P. tauricus* species subgroup we used previously collected sequence data from two mtDNA (16S rRNA and cyt *b*) and three nDNA (MC1R, Pod15b, and Pod55) genes for three specimens of *P. gaigeae*, two of *P. melisellensis*, four of *P. milensis*, 10 of *P. tauricus*, and 15 of *P. ionicus*. This sample selection includes all distinct clades and subclades of the *P. tauricus* species subgroup (Table S1) (Podnar et al., 2014, 2004; Psonis et al., 2017). These data were combined with sequences from 26 specimens of other *Podarcis* species and 12 specimens of other lacertids (*Lacerta, Timon,* and *Gallotia*). These data were included to set age constraints (Table S1). We selected six age constraints using a normal prior distribution, and mean and standard deviation (SD) values as follows: (a) colonization of El Hierro Island (Canary Islands) by the endemic *Gallotia caesaris caesaris* from the neighboring La Gomera Island at 1.12 Mya (Cox et al., 2010; Guillou et al., 1996); mean: 1.05 and SD: 0.20, (b) the divergence time of *P. peloponnesiacus* from *P. cretensis* and *P. levendis* at 5–5.5 Mya (Poulakakis et al., 2005a) corresponding to the separation of Crete from the Peloponnese (Meulenkamp, 1985; Schule, 1993); mean: 5.30 and SD: 0.10, (c) the divergence of *P. lilfordi* from *P. pityusensis* at ~5 Mya (Brown et al., 2008) when their respective island groups split (Terrasa et al., 2004); mean: 5.25 and SD: 0.03, (d) the divergence between the genera *Lacerta* and *Timon* (Čerňanský, 2010) in Lower Miocene (18.1–17.2 Mya); mean: 17.50 and SD: 0.30, (e) the divergence of European *Timon* from the North African lineages at 5.3 Mya (Estes, 1983); mean: 5.30 and SD: 0.7, and (f) the differentiation of the *L. viridis* species group into its constituent species (Venczel, 2006) during the Upper Miocene (9.0–5.3 Mya); mean: 8.70 and SD: 0.50. Sequence alignment was performed as described in Psonis et al. (2017), using MAFFT (v.7; Katoh and Standley, 2013). Divergence times were calculated using the StarBEAST2 (v.0.13.5; Ogilvie et al., 2017) template of BEAST 2 (v.2.4.5; Bouckaert et al., 2014) with the input file being formatted in the BEAUti v.2.4.5 utility included in the same software. The species tree prior category was set to birth-death model, and the uncorrelated lognormal model was used to describe the relaxed clock. Model parameters were unlinked across partitions (tree models for mtDNA genes were linked). Site Models for each partition were calculated using jModelTest2 (Darriba et al., 2012) as follows: 16S rRNA and cyt *b* - GTR + G, MC1R and Pod55 – HKY + I, and Pod15b – HKY + G (four Gamma categories were selected, as well as estimated proportion of invariable sites where applicable). The analysis was run for $5 \times 10^8$ generations with a 5000-step thinning. Results were analyzed in Tracer to assess convergence and ESSs values for all parameters (acceptable values > 200). The –*ln*L was stabilized prior to $5 \times 10^8$, and the first 10% of the 100,000 sampled generations were discarded. The final tree with divergence time estimates was computed in TreeAnnotator v.2.4.5 and visualized using FigTree v.2.4.5 (both in BEAST 2).

### 2.4. Species distribution modelling and niche overlap

A SDM analysis was utilized in order to test a suite of general hypotheses about the factors contributing to the diversity of the of *P. tauricus* subgroup in the Balkans. The analysis was performed for all species of the *P. tauricus* subgroup based on maximum entropy modelling of their geographical distributions. This method combines presence only data with environmental parameters' layers to predict relative probabilities of species' presence in the defined geographic space (Phillips et al., 2006). Occurrence records were obtained from the database of the Natural History Museum of Crete (NHMC). Additional data for *P. melisellensis* were collected from the literature (Podnar et al., 2014, 2004). In total, 427 occurrences were retrieved, from which we retained only one presence point per pixel, so that the final analysis was based on 339 occurrences, 22 of which belonged to *P. gaigeae*, 81 to *P. melisellensis*, 12 to *P. milensis*, 165 to *P. tauricus* and 59 to *P. ionicus*.

To build a species distribution model, environmental layers of climate variables for the present, the last glacial maximum (LGM) (~21 kya) and the last interglacial (LIG) (~120–140 kya) at a 2.5 arc-minutes resolution were downloaded from the WorldClim database website (http://www.worldclim.org/) (Hijmans et al., 2005). Species distributions were estimated using MAXENT (v3.3.3 k; Phillips et al., 2006) based on 10 cross-validation steps. Effectiveness of the model was evaluated using the AUC statistic (Araújo and Guisan, 2006) and the area under the receiver operator curve (ROC) (Phillips et al., 2004). Seven bioclimatic factors from the WorldClim database (bio1,5,6,7,12,14,15) were selected to describe habitat variability and species preferences (Kaliontzopoulou et al., 2008). Niche overlap between species within the subgroup was compared using the relevant indices for niche overlap, *D* and *I*, based on Schoener's *D* (Schoener, 1968) and modified Hellinger *I* (van der Vaart, 1998) distances, respectively, as proposed by Warren et al. (2008), using the ENMtools (Warren et al., 2010).

## 3. Results

### 3.1. Phylogenomic (ddRADseq) relationships and biogeographic analysis

The Illumina sequencing of ddRADseq library including 46 samples resulted in an average of 925,185 good quality reads per sample (after applying a Phred quality filtering threshold of 20) ranging from 43,897 to 3,016,940 reads per sample. The average number of loci per sample for each dataset based on the three different Wclust values (equal to 0.85, 0.90, and 0.95) was 28,304 (range = 11,857–80,468), 30,620 (range = 12,062–84,484), and 44,897 (range = 13,134–133,676) loci, respectively. The number of SNPs present in at least four samples (MinCov = 4, paralogs removed) increased with higher orthology thresholds (20,318, 21,617, and 24,687, respectively for each dataset). However, as we needed to have at least four unique sequences per locus (min_taxa = 4) for phylogenetic purposes, SNP numbers were reduced to 12,560, 12,761, and 11,853 loci, respectively, resulting also in a slightly increase of the percentage of missing data (66.72%, 67.82%, and 71.08%, respectively) when using a higher orthology threshold. By subsampling the datasets and retaining 50% (min_taxa = 7), 25% (min_taxa = 9), and 12.5% (min_taxa = 11) of the initial amount of loci, the amount of gaps/undetermined characters was reduced as expected (56.58%, 56.59%, and 58.40%, respectively for min_taxa = 7, to 50.25%, 50.02%, and 51.25%, respectively for min_taxa = 9, and to 44.85%, 44.45%, and 45.20%, respectively for min_taxa = 11). Summary statistics for all ddRADseq datasets are given in Table 2, whereas various parameters (i.e., sample representation, the percentage of samples per locus, gappyness, and percentage of variable sites per locus) for each Wclust-based dataset and its subsets assembled using the different selected min_taxa filter, are plotted in Figs. S1 and S2.

The mean relative RF distances (a proxy of phylogenetic signal stability) among the 100 ExaML trees produced by each dataset, are

**Table 2**
Summary statistics for the ddRADseq datasets of the *P. tauricus* species subgroup used. Loci and SNPs statistics are in italics and bold, respectively.

| Statistic | Bioinformatics Pipeline step | Wclust = 0.85 | Wclust = 0.90 | Wclust = 0.95 |
|---|---|---|---|---|
| Retained reads that passed quality filtering - NQual (avg ± sd)[a] | pyRAD step 2 (filtering) | 830,692 ± 620,159 | 803,121 ± 601,359 | 764,506 ± 576,221 |
| Mean depth of clusters with depth greater than NQual (avg ± sd) | pyRAD step 3 (within-sample clustering) | 55.7 ± 26.5 | 56.3 ± 26.4 | 58.1 ± 27.7 |
| Number of loci per sample (avg ± sd) | pyRAD step 5 (consensus sequences) | *28,304 ± 11,648* | *30,620 ± 12,671* | *44,987 ± 21,211* |
| Number of loci per sample with depth greater than NQual (avg ± sd) | pyRAD step 5 (consensus sequences) | *9,539 ± 3,361* | *9,974 ± 3,596* | *10,370 ± 3,786* |
| Number of loci per sample with depth greater than NQual and paralogs removed (avg ± sd) | pyRAD step 5 (consensus sequences) | *8,580 ± 2,999* | *9,062 ± 3,253* | *9,857 ± 3,580* |
| Number of sites across loci per sample with depth greater than NQual and paralogs removed (avg ± sd) | pyRAD step 5 (consensus sequences) | 761,718 ± 266,456 | 804,845 ± 289,044 | 875,893 ± 318,193 |
| Number of polymorphic sites across loci per sample with depth greater than NQual and paralogs removed (avg ± sd) | pyRAD step 5 (consensus sequences) | 2,258 ± 1,302 | 2,431 ± 1,389 | 2,577 ± 1398 |
| Number of loci with at least MinCov samples containing data[b] | pyRAD step 6 (across-sample clustering) | *21,906* | *23,173* | *25,895* |
| Number of loci with at least MinCov samples containing data and paralogs removed | pyRAD step 7 (alignment and paralog filtering) | *20,318* | *21,617* | *24,687* |
| Total variable sites | pyRAD step 7 (alignment and paralog filtering) | 133,930 | 124,539 | 95,575 |
| Sampled unlinked SNPs | pyRAD step 7 (alignment and paralog filtering) | **18,391** | **19,361** | **21,412** |
| Sampled unlinked bi-allelic SNPs | pyRAD step 7 (alignment and paralog filtering) | **13,214** | **13,789** | **14.065** |
| Number of loci after Min_taxa = 4 filtering | Subset selection | *12,560* | *12,761* | *11,853* |
| Number of loci after Min_taxa = 7 filtering | Subset selection | *7,531* | *7,126* | *5,062* |
| Number of loci after Min_taxa = 9 filtering | Subset selection | *5,100* | *4,626* | *2,683* |
| Number of loci after Min_taxa = 11 filtering | Subset selection | *3,289* | *2,862* | *1,240* |

[a] NQual equals to 14, 9, and 5 for the 0.85, 0.90, and 0.95 Wclust filtered datasets, respectively.
[b] MinCov equals to 4 for all three Wclust filtered datasets.

shown in Table S3. The corresponding pairwise mean relative RF distances between the best scoring ExaML trees inferred from the 12 different datasets are given in Table S4. It is worth noting that only four distinct best-scoring ExaML trees were obtained from these 12 datasets, with one of them (Fig. 2A) being the most consistent across most of the datasets (i.e. in 8 datasets: 0.85 and 0.90 clustering thresholds and all min_taxa filters). The remaining three topologies are presented in Fig. S3. We chose the dataset with Wclust = 0.85 for downstream analyses based on phylogenetic signal stability and amount of missing data for min_taxa = 4 (since all subsets of Wclust = 0.85 had the same RF distance). This dataset was used to reconstruct phylogenies with the ML and the BI methods. The ML analysis completed after 150 bootstrap pseudo-replicates, controlled by the bootstopping option of autoMRE (Pattengale et al., 2010). The BI analysis that converged after 2,000,000 generations according to the sdsfConvergence option, resulted in high effective sample sizes (ESS > 631) and *ln*L = −2,350,840.74. The extended Majority Rule Consensus tree computed from the final 8000 trees is in agreement with the ML tree, and is presented in Fig. 2A. According to the consensus between the ML and BI methods inferred phylogeny, five major clades were revealed, each corresponding to one of the five species of the *P. tauricus* species subgroup. The relationships among them are fully resolved, with *P. melisellensis* being the sister taxon to all the rest. Two subsequent cladogenetic events led to *P. milensis* and *P. gaigeae,* whereas *P. tauricus* and *P. ionicus* were the last clades that diverged, and have a sister group relationship. Within the clade of *P. ionicus* four subclades were recognized, with one (subclade *a*) originating from the south Ionian Sea (Zakynthos and Kefalonia Islands), one (subclade *e*) from the western part of Pindos Mt., one (subclades *b* and *d*) from southeastern Peloponnese and west central Greece, and a final one (subclade *c*) from northeastern Peloponnese (see Fig. 1 for locations mentioned).

The exhaustive quartet search of SVDQuartets method resulted in 163,185 quartets, which were used to infer the SNP based species tree, whose topology matches the one inferred from the concatenated dataset (Fig. 2A).

Biogeographic reconstructions for 17 major nodes are presented in Fig. 2A. All reconstructed areas and detected biogeographic events had 100% statistical support. This analysis suggests that the ancestral form of the *P. tauricus* species subgroup was distributed across the southern Balkans and its biogeographic history was the result of several recurring vicariance and dispersal events (six and two, respectively). The divergence events leading to the splits among the *P. melisellensis*, *P. milensis*, *P. gaigeae*, *P. tauricus*, and *P. ionicus* were likely due to vicariance, as the splits leading to the differentiation of the *P. ionicus* subclades *a* and *e*. In contrast, separation of the three *P. ionicus* subclades *b*, *c*, and *d* were likely due to dispersal.

The STRUCTURE analysis based on the ddRADseq dataset resulted in seven clusters with two equally likely solutions/modes (bimodality), as shown in Fig. 2B. In both cases, five of the clusters include samples from previously recognized taxonomic groups (*P. gaigeae, P. milensis, P. melisellensis*, *P. tauricus*, and subclade *c* of *P. ionicus*, respectively; Fig. 2A). The bimodality pertains to the remaining two subclades of *P. ionicus*. The members of the *P. tauricus* species subgroup were partially discriminated at the species level according to the DAPC analysis, using five discriminant factors (Fig. S6).

### 3.2. Population genetics using microsatellites data

Three loci (Pb47, Pod3, and Pod8) were discarded from the microsatellites dataset either due to unsuccessful genotyping or to being monomorphic. Furthermore, 48 specimens were discarded (Table S1) from subsequent analyses due to missing data (i.e., less than half of the loci were genotyped). Thus, the final analyses were performed using 361 specimens (52*P. gaigeae*, eight *P. melisellensis*, 53*P. milensis*, 177*P. tauricus*, and 71*P. ionicus*) and 14 microsatellite polymorphic loci. None of the microsatellite loci showed negative $F_{IS}$ values. Large allele

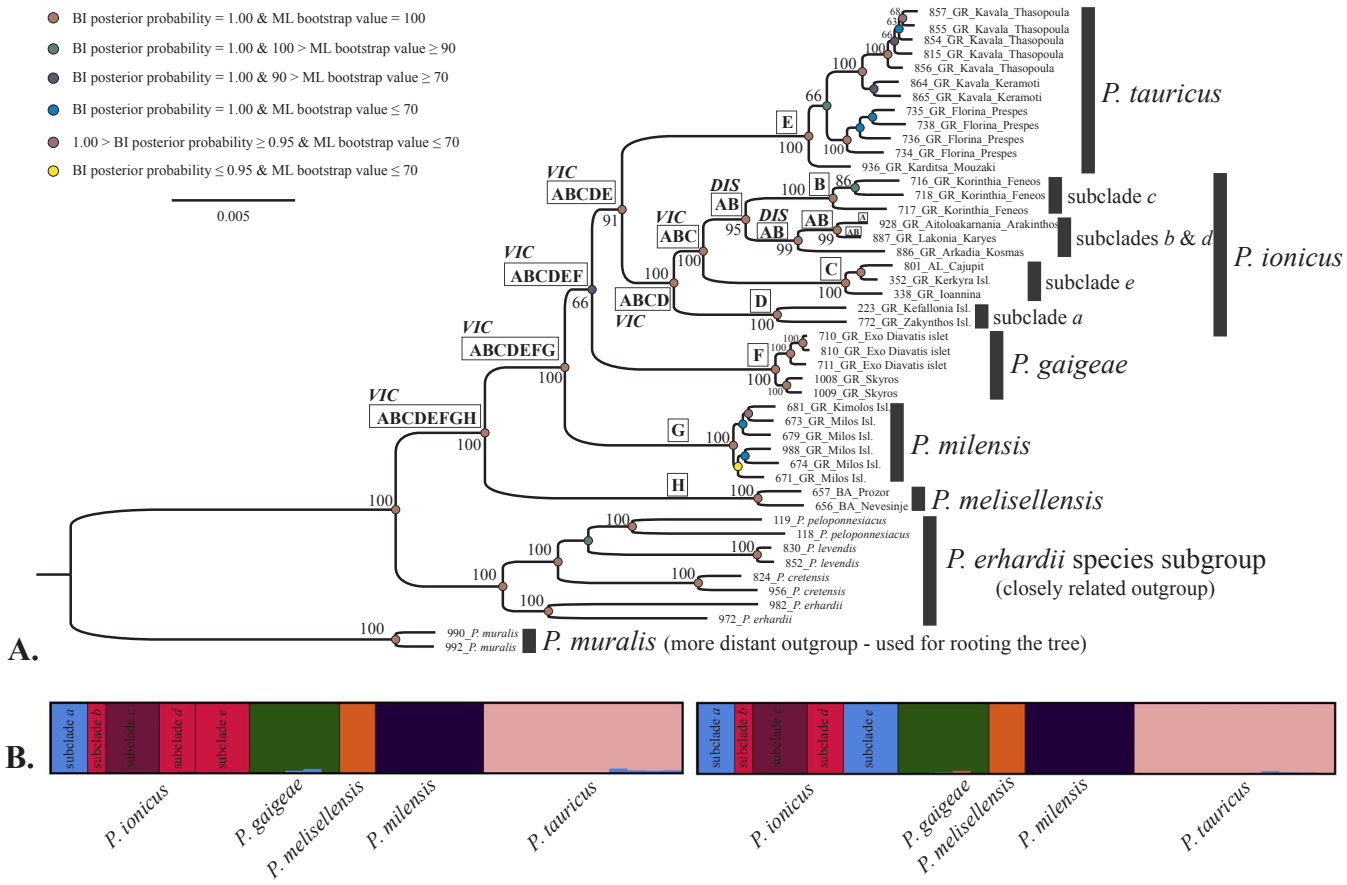


**Fig. 2.** (A) Bayesian Inference phylogenomic tree of the *P. tauricus* species subgroup based on ddRADseq data using the clustering threshold of 0.85 and min_taxa filter of 4. The colors of the nodes correspond to different combinations of posterior probabilities (BI method) and bootstrap values (ML method) as indicated in the inlaid table at the upper left corner. Numbers near the nodes correspond to the statistical support (bootstrap values) of the SNP based species tree inferred using the SVDQuartets method, which resulted in the same topology. The names of subclades (*a* to *e*) match with the corresponding subclades revealed in chronophylogenetic analysis (see Fig. 3) and in Psonis et al. (2017). The capital letters within the squares next to the nodes correspond to reconstructed ancestral distributions inferred by the DEC biogeographic analysis, as follows: A – west central continental Greece, B – Peloponnese, C – northwestern continental Greece and southwestern Albania, D – south Ionian islands, E – Eastern Balkans and eastern Europe (Moldavia, Ukraine, and Crimea), F – Skyros Island group, G – Milos Island group, H – Northwestern Balkans. The capital italicized letters indicate vicariance (VIC) and dispersal (DIS) events detected by the DEC analysis. All reconstructed areas and biogeographic events had 100% statistical support. (B) The estimated population structure (two possible modes) of the *P. tauricus* species subgroup using the ddRADseq dataset. The Q value corresponds to the percentage of estimated assignment of the individual to each one of the *K* clusters.

**Table 3**
Population genetics descriptive statistics for all data and for each species of the *P. tauricus* subgroup (excluding *P. melisellensis* due to small number of samples) based on microsatellites data.

| Loci | $N_A$[a] | All data | | | P. tauricus | | | P. ionicus | | | P. gaigeae | | | P. milensis | | |
|---|---|---|---|---|---|---|---|---|---|---|---|---|---|---|---|---|
| | | $H_o$[b] | $H_e$[c] | $F_{IS}$[d] | $H_o$ | $H_e$ | $F_{IS}$ | $H_o$ | $H_e$ | $F_{IS}$ | $H_o$ | $H_e$ | $F_{IS}$ | $H_o$ | $H_e$ | $F_{IS}$ |
| B6 | 28 | 0.722 | 0.921 | 0.217 | 0.661 | 0.837 | 0.211 | 0.729 | 0.947 | 0.232 | 0.730 | 0.914 | 0.204 | 0.906 | 0.909 | 0.004 |
| C9 | 31 | 0.417 | 0.763 | 0.454 | 0.263 | 0.410 | 0.359 | 0.426 | 0.930 | 0.544 | 0.490 | 0.739 | 0.339 | 0.885 | 0.893 | 0.001 |
| Lv3-19 | 22 | 0.732 | 0.919 | 0.204 | 0.728 | 0.889 | 0.181 | 0.618 | 0.848 | 0.273 | 0.773 | 0.923 | 0.164 | 0.846 | 0.911 | 0.072 |
| Lv4-72 | 26 | 0.629 | 0.883 | 0.291 | 0.529 | 0.719 | 0.2641 | 0.642 | 0.923 | 0.306 | 0.727 | 0.924 | 0.215 | 0.823 | 0.895 | 0.081 |
| Pb10 | 36 | 0.655 | 0.938 | 0.302 | 0.715 | 0.922 | 0.225 | 0.191 | 0.384 | 0.504 | 0.686 | 0.854 | 0.198 | 0.708 | 0.941 | 0.250 |
| Pb50 | 15 | 0.329 | 0.683 | 0.609 | 0.174 | 0.386 | 0.549 | 0.157 | 0.674 | 0.768 | 0.520 | 0.735 | 0.295 | 0.189 | 0.595 | 0.685 |
| Pli4 | 34 | 0.726 | 0.949 | 0.235 | 0.748 | 0.931 | 0.197 | 0.672 | 0.942 | 0.288 | 0.750 | 0.947 | 0.211 | 0.729 | 0.898 | 0.189 |
| Pm16 | 24 | 0.776 | 0.904 | 0.151 | 0.819 | 0.857 | 0.045 | 0.717 | 0.876 | 0.183 | 0.704 | 0.854 | 0.177 | 0.769 | 0.889 | 0.136 |
| Pm27 | 36 | 0.616 | 0.918 | 0.329 | 0.716 | 0.860 | 0.168 | 0.449 | 0.927 | 0.517 | 0.680 | 0.882 | 0.231 | 0.461 | 0.886 | 0.481 |
| Pmeli02 | 45 | 0.588 | 0.941 | 0.375 | 0.609 | 0.922 | 0.340 | 0.364 | 0.955 | 0.623 | 0.600 | 0.921 | 0.352 | 0.721 | 0.947 | 0.241 |
| Pmeli19 | 45 | 0.781 | 0.965 | 0.191 | 0.741 | 0.918 | 0.193 | 0.735 | 0.949 | 0.227 | 0.844 | 0.902 | 0.065 | 0.923 | 0.948 | 0.027 |
| Pod1A | 20 | 0.136 | 0.493 | 0.724 | 0.045 | 0.320 | 0.860 | 0.191 | 0.384 | 0.504 | 0.038 | 0.146 | 0.7381 | 0.417 | 0.597 | 0.304 |
| Pod1B | 23 | 0.329 | 0.683 | 0.518 | 0.214 | 0.310 | 0.310 | 0.380 | 0.784 | 0.517 | 0.333 | 0.533 | 0.378 | 0.674 | 0.943 | 0.287 |
| Pod2 | 32 | 0.495 | 0.819 | 0.395 | 0.378 | 0.494 | 0.235 | 0.596 | 0.923 | 0.356 | 0.762 | 0.869 | 0.126 | 0.706 | 0.915 | 0.230 |
| Average across all loci | | 0.566 | 0.841 | | 0.524 | 0.698 | | 0.491 | 0.923 | | 0.617 | 0.796 | | 0.697 | 0.869 | |

[a] For all data.
[b] $H_o$: observed heterozygosity.
[c] $H_e$: estimated expected heterozygosity (Nei, 1987).
[d] $F_{IS}$: Inbreeding index ofWeir and Cockerham (1984).

dropout was not observed in any of the 14 loci. Average number of alleles equals to 29.8, ranging from 15 (Pb50) to 45 (Pmeli02 & Pmeli09; Table 3).

Relatedness analyses suggested that the proportion of putative first-order related individuals found was < 1%. No parent–offspring relationship was statistically supported and only eight full siblings were present (results not shown).

The first step of the hierarchical analysis with STRUCTURE led to $K = 2$, with one cluster containing samples of *P. tauricus* and the second containing the remaining species. The second step led to $K = 3$ for the first cluster and $K = 4$ for the second one. In the first case, the three clusters correspond to: (i) western range of *P. tauricus* that incudes Albania, Bulgaria, FYROM, Greece, Hungary, Romania, Serbia and Turkey (final cluster 'tauricus 1'), (ii) eastern range of *P. tauricus* that consists of the Crimean Peninsula, Ukraine and Moldova (final cluster 'tauricus 2'), and (iii) Thasopoula islet (final cluster 'tauricus 3'). In the second case, the four clusters correspond to: (i) *P. ionicus* subclade *e* (final cluster 'ionicus 1'), (ii) *P. ionicus* subclades *c* and *d* (final cluster 'ionicus 1'), (iii) *P. melisellensis* and *P. milensis* ('melisellensis-milensis'), and (iv) *P. gaigeae* ('gaigeae'). The third hierarchical STRUCTURE analysis step was applied only to clusters with > 20 samples, so that there is sufficient information for the detection of population structure signs (if any). All led to $K = 1$, except for three cases ('ionicus 2', 'melisellensis-milensis', and 'gaigeae') that showed population substructure with $K = 3$ (bimodality issues), $K = 2$ (final clusters 'melisellensis' and 'milensis'), and $K = 2$ (final clusters 'gaigeae 1' and 'gaigeae 2'), respectively. Finally, the fourth STRUCTURE step that was conducted only for one of the clusters ('milensis') resulted in $K = 1$. The results of the hierarchical STRUCTURE analysis are given in Fig. 3B and Fig. S4A. A detailed description of these results is provided in the Supporting Information (Supporting Figures PDF, Comment S1A). The Ho, He, and $F_{IS}$ values for each hierarchical STRUCTURE cluster are given in Tables S5 and S6. For the majority of the resulting clusters the $F_{IS}$ values were positive. Departures from HW equilibrium were observed for most of the loci in each cluster ($P < 0.00001$ after Bonferroni correction). The number of loci with null alleles ranged from two to nine, whereas large allele dropout was not observed for any locus in any cluster. The pairwise F*st* values between the final clusters are listed in Table S7. Migration analyses suggests low migration rates ($m < 0.025$) between clusters, except for those of 'tauricus 1' to 'tauricus 2' ($m = 0.17$), and of 'milensis' to 'melisellensis' ($m = 0.21$), where unidirectional migration was identified. The results between the two separate runs were consistent (Table S8).

Eight discriminant functions (DFs) better reflected the observed differences among clusters while minimizing variation within clusters according to the DAPC analysis (Fig. S5). The members of the *P. tauricus* species subgroup were discriminated at the species level.

The infinite allele model (IAM), TPM and stepwise mutation model (SMM) were used to test for population bottlenecks. Populations exhibiting a significant heterozygosity excess are considered to have gone through a genetic bottleneck. Based on the Wilcoxon test (which is considered to be more reliable than the sign test and standardized differences test), the SMM and TPM models did not show significant results for population bottleneck in any cluster ($p > 0.05$), except for those of 'ionicus 1' (under SMM), 'tauricus 1' (under SMM), and 'tauricus 2' (under both TPM and SMM) (Table S9). The same test showed a significant excess of heterozygosity in 'tauricus_3', 'milensis', and 'gaigeae 2' clusters under the IAM ($p < 0.05$) model. However, this is not necessarily indicative of true heterozygosity excess, as the IAM is considered less appropriate for microsatellites than the SMM (Shriver et al., 1993).

Demographic expansions were detected by the intralocus k-test on the 14 microsatellite loci for three final hierarchical STRUCTURE clusters (i.e., 'gaigeae 2', 'ionicus 1', and 'tauricus 2'; Table S10). By contrast, the interlocus g-test was not significant in any case, as the observed g statistic was higher than the five-percentile cut-off value. However, g-tests are sensitive to variation in mutation rates among loci (King et al., 2000). This could explain the non-significance of the g-tests herein, given the extensive variability in allele size range and allele numbers among the different microsatellite loci (Table 3).

### 3.3. mtDNA haplotype networks and historical demographics

The mtDNA haplotype networks for each major phylogenetic clade and subclade of the *P. tauricus* species subgroup are shown in Figs. S7–S12. In the case of *P. melisellensis,* we show the haplotype network from Podnar et al. (2004) due to the limited number of samples in our study compared to the one used therein. The highest genetic diversity is observed within *P. ionicus* and *P. melisellensis* (Table S11), whereas the lowest within *P. tauricus* and *P. gaigeae*. The mtDNA demographic analyses resulted in a variety of patterns (Table S12, Figs. S13 and S14). In some cases, there was a clear indication of demographic expansion during the past (i.e., *P. tauricus* and subclade *e* of *P. ionicus*), or of demographic equilibrium (i.e., subclades *a* and *b* of *P. ionicus*). According to the Bayesian Skyline Plots (Fig. S13), during the past, *Ne* for *P. gaigeae* and *P. melisellensis* remained quite stable, experienced a small increase for *P. milensis* and progressively increased for *P. tauricus* . In contrast, a recent sudden *Ne* reduction, followed by a sudden expansion, was detected in *P. ionicus* and in subclade *e* of the same species.

### 3.4. Divergence time estimation

The chronophylogenetic analysis on the five gene dataset resulted in high posterior ESS values (> 209) for all parameters, and convergence was reached prior to $5 \times 10^8$ generations ($lnL = -11{,}827.66$). According to the inferred dates (Fig. 3), the *P. tauricus* species subgroup started to diversify in the Messinian (Late Miocene) around 5.55 Mya Mya with the divergence of *P. melisellensis*. The other three major cladogenetic events occurred in the early Pliocene (4.71–3.88 Mya).

### 3.5. Species distribution modelling and niche similarity

The model yielded AUC scores > 0.92, indicating a good model performance (Fig. S15). The overall estimated distribution patterns of the focal species were consistent with their actual distribution. The most important climatic parameter was the annual range of temperature for *P. gaigeae*, *P. milensis*, and *P. tauricus*, the minimum temperature of the coldest month for *P. melisellensis,* and precipitation seasonality for *P. ionicus* (Table S13). However, the projection of the models over the LGM (Fig. S16) produced a predicted distribution different from their current one (Fig. 4). Significant range contractions of all species were observed during the LGM compared to the present, except for *P. milensis*. For *P. ionicus*, the potential distribution was smaller in LGM, whereas during the LIG it was limited mostly to regions of low elevation and to coastal areas.

The niche similarity analyses (Schoener's *D*) showed that there is no niche overlap between any pair of the focal taxa, except for a low overlap for the *P. gaigeae* – *P. milensis* niche. For more details see Table S14. The Hellinger's *I* suggested low niche overlap between *P. tauricus* – *P. ionicus* and *P. ionicus* – *P. melisellensis*, and moderate overlap between *P. gaigeae* – *P. milensis*.

## 4. Discussion

### 4.1. Phylogenomic relationships within the P. tauricus species subgroup

Although previous phylogenetic studies, based either on nuclear and/or mitochondrial genes, supported the monophyly of the species, phylogenetic relationships among them remained ambiguous (Poulakakis et al., 2005a, 2005b; Psonis et al., 2017). The ddRADseq data clarified these relationships within the *P. tauricus* species subgroup and produced a completely resolved phylogeny at the species level

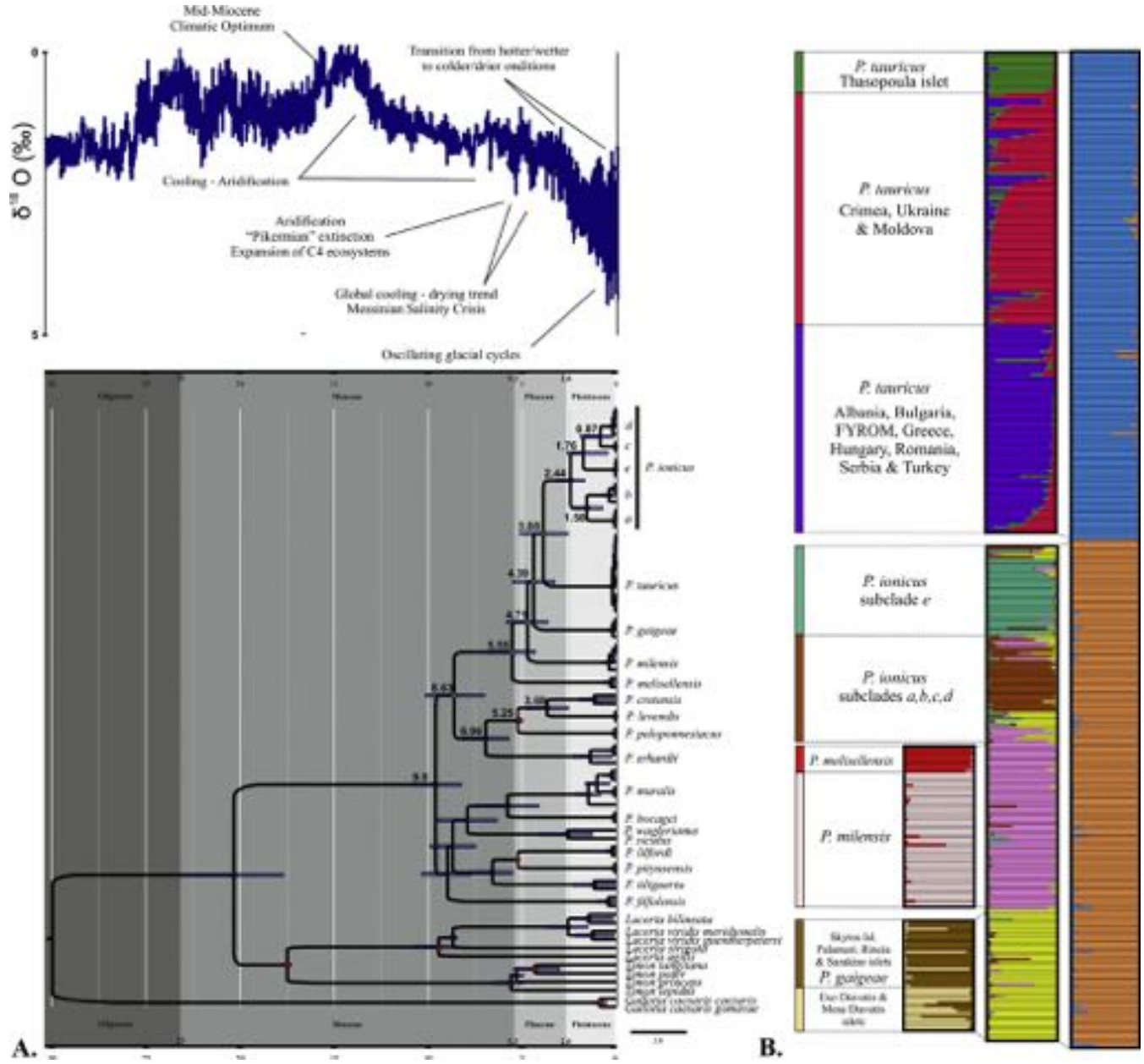


**Fig. 3.** (A) The calibrated starBEAST2 species tree of the *P. tauricus* species subgroup distributed in the Southern Europe, from the chronophylogenetic analysis based on three nuclear (Pod55, Pod15b, and *MC1R*) and two mitochondrial gene fragments (16S rRNA and cyt *b*). The black and grey circles on the nodes correspond to absolute (posterior probability = 1.00) and very good (0.95 < posterior probability < 1.00) statistical support, whereas the absence of a circle indicate low statistical support. With red colors are the nodes used as calibration points. The numbers on clades of interest constitute the divergence times in Mya, whereas the horizontal bars show the uncertainty (95% HPD) in molecular dating. The bar at the bottom measures Mya. At the top of the Figure, a graphical representation of temperature fluctuations during the past ~35 My, as depicted from deep-sea oxygen isotope records (redrawn after Zachos et al., 2001). (B) The estimated population structure of the *P. tauricus* species subgroup after four steps of the hierarchical STRUCTURE analysis using microsatellites data. Every individual is represented by a thin horizontal line that consists of *K* numbers of colors. The Q value corresponds to the percentage of estimated assignment of the individual to each one of the *K* clusters.

(Fig. 2**)**. Within this subgroup, *P. melisellensis* branches off first, *P. milensis* diverged next, and *P. gaigeae* is the sister taxon to *P. tauricus* and *P. ionicus*.

The genomic data also revealed a well-supported within species structure for *P. tauricus* and *P. ionicus* (Fig. 2). Within the former, although three lineages were observed, the low representation of each species in the ddRADseq dataset prevents to assess the validity of this grouping. For *P. ionicus* this study suggests the occurrence of four subclades, a finding that partially agree with that of a previous study (Psonis et al., 2017). According to the later *P. ionicus* includes five subclades (Figs. S10–S12). These include subclade *a* from south Ionian Islands, subclade *b* from western central Greece (Trichonida lake), subclade *c* from northeastern Peloponnese, subclade *d* from central and southeastern Peloponnese, and subclade *e* from western Peloponnese and northwestern Greece – southwestern Albania. However, subclade *b* and *d* are not distinct in the genomic tree of the present study, in contrast to Psonis et al. (2017) where subclade *b* appears as a separate subclade with a sister group relationship with subclade *a*.

### 4.2. Population structure and demographic events

The hierarchical structuring analyses on microsatellites dataset

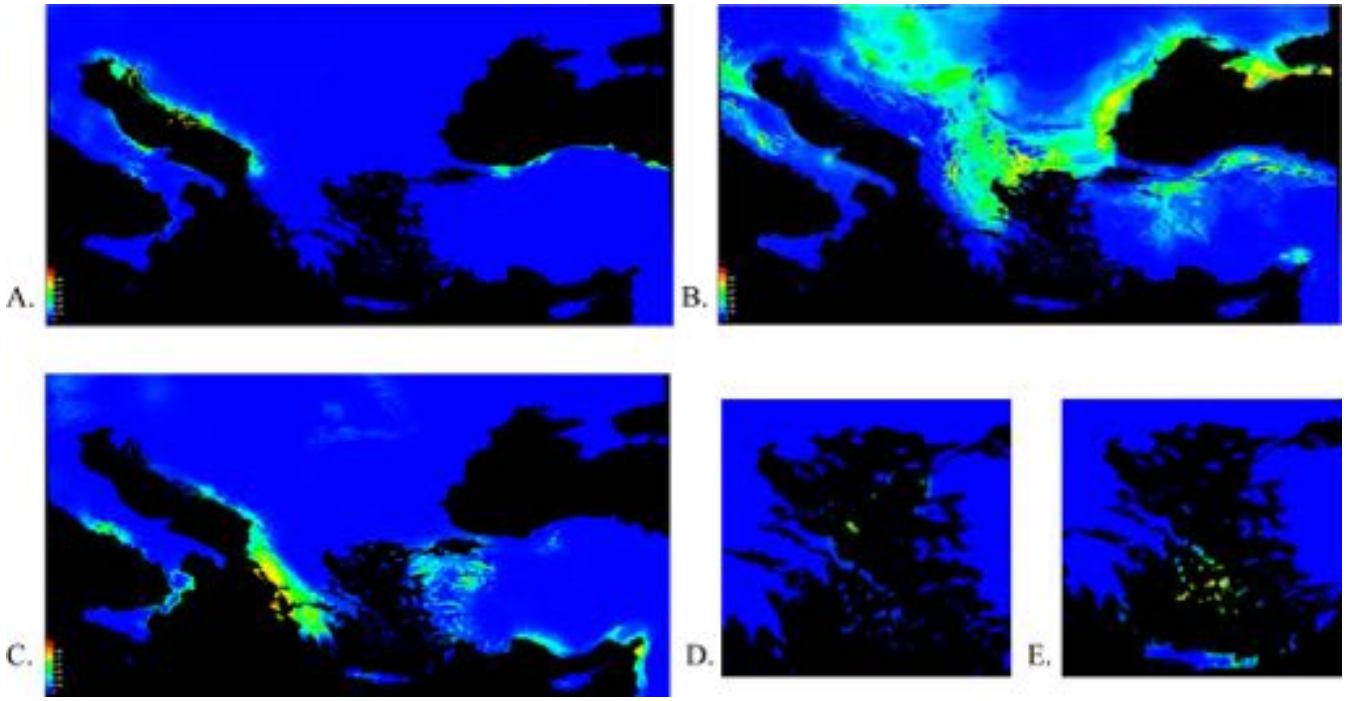


**Fig. 4.** Species Distribution Modelling using the MaxEnt model for the focal species (A: *P. melisellensis*, B: *P. tauricus*, C: *P. ionicus*, D: *P. gaigeae*, E: *P. milensis*). The SDM projection correspond to the current time period.

revealed nine clusters, which were approximately geographically consistent. One of them ('ionicus 2'; *P. ionicus* subclades *a-d*) was further subdivided although with bimodality issues. These final clusters support the differentiation of *P. tauricus* species subgroup into five species and reveal further sub-structuring within them. The pattern of population structure based on the SNPs is in accordance with the above findings, albeit no further sub-structuring within species was observed, except for *P. ionicus* that, again, showed bimodality issues. Sudden expansion was detected in the microsatellites clusters of 'ionicus 1' (*P. ionicus* subclade *e*), 'tauricus 1' (*P. tauricus* from Thasopoula islet, North Aegean, Greece), and 'tauricus 2' (*P. tauricus* from the Crimean Peninsula, Moldova, and Ukraine), with the first and the third showing signs of sudden expansion during the recent past, possibly following a bottleneck. The above findings are also concordant with the demographic analyses based on mtDNA data. Moderate unidirectional migration was observed from 'melisellensis' (in the present study, only from Montenegro and Bosnia-Herzegovina) to 'tauricus 1'. However, the large geographical distance between the two coupled with the fact that these are different species makes this scenario implausible, suggesting that shared ancient allele polymorphisms rather than current migration might be a better explanation for the observed pattern. In contrast, unidirectional migration from 'gaigeae 1′ (Skyros Isl.; main island of the archipelago) to the nearby located 'gaigeae 2' (Mesa Diavatis and Exo Diavatis satellite islets) is highly plausible, given the proximity of the two and the size difference among the respective islands.

### 4.3. Phylogeographic hypothesis for P. tauricus species subgroup

Ecological competition among the Balkan *Podarcis* species has been proposed as one of the main drivers of their evolutionary history (Oliverio et al., 2000; Poulakakis et al., 2005a, 2005b). Either the ancestral form of *P. erhardii* species subgroup was the first to colonize the Balkan Peninsula and the ancestor of *P. tauricus* subgroup arrived later (Oliverio et al., 2000) or the reverse (Poulakakis et al., 2005a, 2005b). These two species subgroups are ecologically differentiated, with *P. erhardii* inhabiting more rocky habitats and *P. tauricus* usually found in areas with low vegetation (Valakos et al., 2008). Nevertheless, both scenarios have several shortcomings. According to the first, while the ancestral form of *P. tauricus* dispersed in the Aegean it would have colonized only two island groups (Skyros and Milos) leading to the modern *P. gaigeae* and *P. milensis*, respectively. According to the second, the two species subgroups that today are ecologically distinct, would have been competitors so that the ancestor of *P. erhardii* would have displaced the ancestor of *P. tauricus*. However, given that the spatial and temporal patterns of ecological diversification among those species groups remain ambiguous, it is not safe to consider competition between the ancestral forms as the main force of *Podarcis'* differentiation in the Balkan Peninsula. Since a proper phylogeographic scenario should take into account several possible drivers of differentiation, we present and discuss below a revised phylogeographic scenario from the Late Miocene to the present, taking into account a series of historical and ecological factors. The scenario is shown in a series of maps in Fig. 5.

### 4.4. Species divergence in the Late Miocene and Early Pliocene

The differentiation of *Podarcis* started in the Upper Miocene (~9.60 Mya) following the tectonic collision of the Adriatic-Apulian mass with Eurasia at ~14–15 Mya (Steininger and Rögl, 1984). The intense orogenetic activity during this period was likely the main factor driving the genetic differentiation within *Podarcis*, which colonized the Balkan Peninsula from the western parts of Europe (Oliverio et al., 2000). The differentiation of the Balkan species group started at 8.63 Mya, which is two million years earlier than previously estimated (10.6 Mya; Poulakakis et al., 2005a, 2005b), which were was inferred using a concatenated mtDNA dataset and not a multilocus species tree, as in the present study. The new divergence time coincides with the formation of the Mid-Aegean Trench (MAT; Creutzburg, 1963; Dermitzakis and Papanikolaou, 1981). The absence of *Podarcis* from Anatolia and the east Aegean islands could be an indication that the colonization of the southern Balkans occurred after the formation of MAT. This period coincides with global cooling and aridification (Fig. 3A), a major expansion of dry zones, and replacement of forests by woodland and

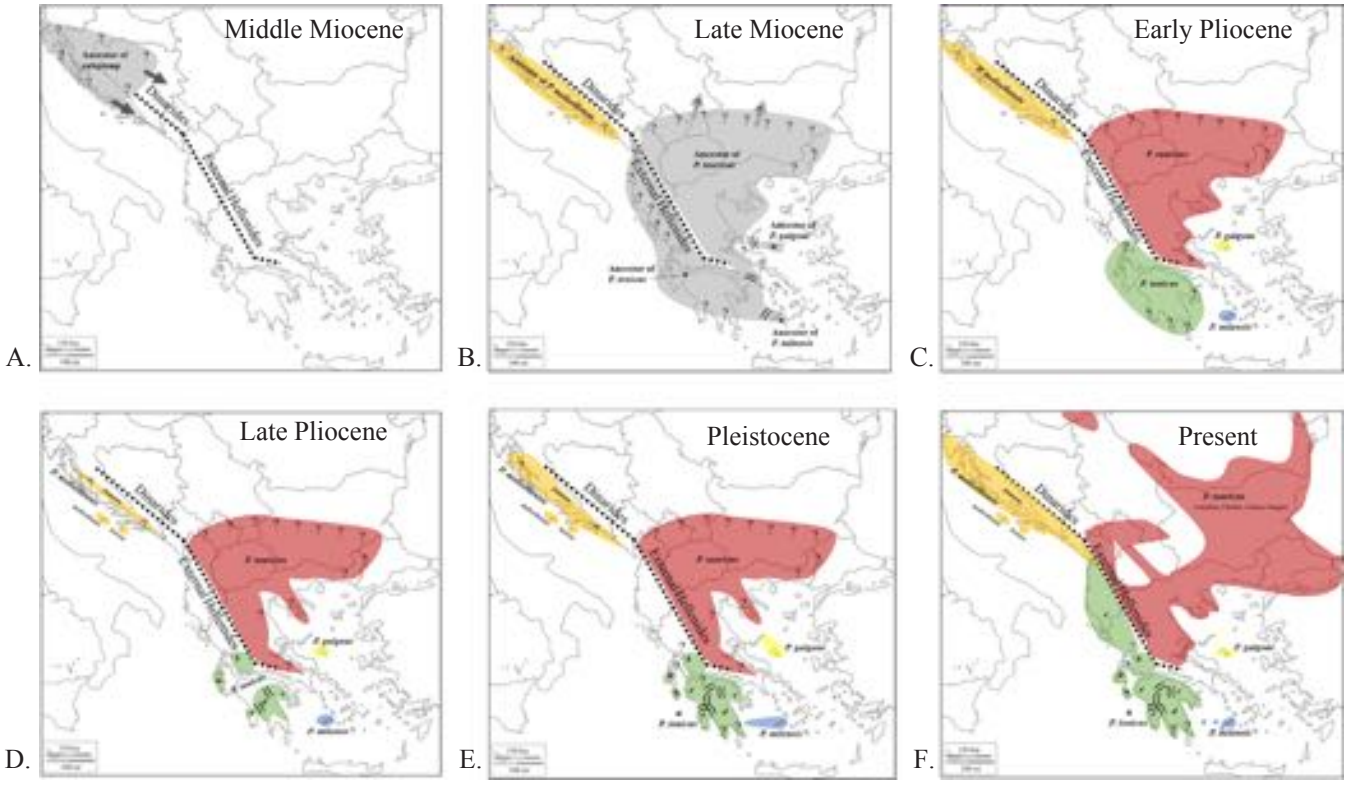


**Fig. 5.** The proposed phylogeographic scenario of the *P. tauricus* species subgroup distributed in the Southern Europe described in a series of six maps from the Late Miocene to the present.

grasslands (Middle and Late Miocene), particularly in mid-latitudes (Crowley and North, 1991; Potts and Behrensmeyer, 1992). The exact colonization route (from the east, the west or from both sides of the Dinarides and Pindos Mts.) followed by the *P. tauricus* species subgroup is difficult to infer. The Pindos mountain range (Fig. 1A), could have had an important filtering effect for the species' dispersal to the south, as observed in other amphibians and reptiles [*Lacerta viridis* and Adriatic lineage of *L. billineata* (Marzahn et al., 2016; Mayer and Beyerlein, 2001; Sagonas et al., 2014), *Natrix natrix* (Kindler et al., 2013), *N. tessellata* (Guicking et al., 2009), *Pelophylax epeiroticus* (Akın et al., 2010; Lymberakis et al., 2007), and *Vipera ammodytes* (Ursenbacher et al., 2008)]. During the Messinian Salinity Crisis (MSC = 5.96–5.33 Mya, Late Miocene) (Hsü, 1972; Jolivet et al., 2006; Kenneth et al., 1977; Krijgsman et al., 1999) the Mediterranean islands became mountains surrounded by steppes or saline deserts, enabling over land dispersal for several organisms (Poulakakis et al., 2014 and references therein). Irrespective of the time when the ecological differentiation of *P. tauricus* and *P. erhardii* subgroups took place, both subgroups started to diverge in the Messinian. The diversification of the *P. tauricus* species subgroup coincides with the end of MSC (at ~5.55 Mya), when *P. melisellensis* split (Fig. 3A). Its exclusive presence in the Dalmatic coasts, in combination with the vicariance event inferred from this study's biogeographic analysis (Fig. 2), suggests that its divergence could have occurred in that area. The uplift of the Dinarides mountain range, which was initiated in the Middle Miocene (Kuhlemann, 2007) at ~8 Mya, in conjunction with the remarkable alterations in the Dalmatian coasts during the MSC (Popov et al., 2004), could have caused a vicariance event that lead to the isolation of the ancestral *P. melisellensis* population. Subsequent events that might have further promoted the divergence of the subgroup at the species level occurred in the early Pliocene (4.71–4.39 Mya) (Fig. 3A). During the late Miocene, southern Greece consisted of two small peninsulas forming a fork (Creutzburg, 1963; Dermitzakis and Papanikolaou, 1981); one in the southwest, corresponding to the present area of the Peloponnese and Crete, and another in the southeast, corresponding to the east central Greece and the Cyclades of today (Fig. 1A). The reopening of the Mediterranean Sea after the end of the MSC, leading to the refilling of the basin, caused the permanent isolation of Crete from Anatolia, the Peloponnese, and the Cyclades, a fact also supported by additional evidence regarding faunal evolution on the island (Dermitzakis, 1990). The exact ancestral distribution of the *P. tauricus* species subgroup at that time is difficult to determine. One of the most parsimonious hypotheses is that the ancestral form of this subgroup was distributed in the areas that are now occupied by the present species (*P. gaigeae, P. milensis, P. tauricus,* and *P. ionicus*). Then this area became permanently subdivided into four isolated areas in the early Pliocene (Fig. 5), including areas that presently correspond to (a) the island group of Skyros, (b) the island group of Milos, (c) the (at that time united) areas of Peloponnese, western central Greece, and the Ionian Islands, and (d) the area east of Pindos Mt. (see Fig. 1A for current geographic locations). According to the biogeographic analysis, vicariance events were the main drivers of diversification. However, several factors could have contributed to this particular distribution pattern, including historical and ecological constraints acting independently or synergistically. Historical factors (vicariance) include the isolation of the areas inhabited by the ancestors of the species *P. ionicus*, *P. gaigeae*, *P. milensis*, and *P. tauricus* during the MSC. High temperatures and lack of suitable habitats for taxa preferring low vegetation could be considered as important ecological constraints. In any case, competition between the focal subgroup and the *P. erhardii* subgroup, today adapted to more xeric environments, should not be excluded.

Overall, it seems that the first phase (differentiation among species) of the evolutionary history of the *P. tauricus* species subgroup was shaped by several geomorphological alterations and climatic oscillations that happened at the end of late Miocene. These events, at the end of the MSC, have been considered as the major differentiation drivers enhancing allopatric speciation also for other insular populations of Aegean species, such as the lizards *Ablepharus kitaibelii* (Skourtanioti

et al., 2016), *P. erhardii* (Poulakakis et al., 2005b), and *Lacerta trilineata* (Sagonas et al., 2014).

### 4.5. Within species differentiation during the Pliocene and Early Pleistocene

During the Pliocene, most of the Cyclades islands, including Milos island group, as well as the Skyros archipelago (Fig. 1A) became permanently isolated from the Peloponnese and continental Greece, respectively (Dermitzakis, 1990, 1989). The mountain range of Pindos has probably been an important biogeographic barrier between western Greece / Peloponnese and eastern Greece. Based on our estimations, intra-specific differentiation occurred in the Pliocene for *P. ionicus* and in the Pleistocene for *P. milensis, P. gaigeae, P. tauricus*, and *P. melisellensis*. Several tectonic faults that were activated during the Pliocene in the Corinthian Gulf caused the isolation of the Peloponnese from continental Greece, whereas subsequent tectonic events separated Zakynthos and Kefalonia islands (Fig. 1A) from the Peloponnese (Creutzburg, 1963; Zelilidis et al., 1998). The isolation of the Peloponnese from continental Greece has been assumed to be the main cause of allopatric differentiation and speciation for several species, including the lizards *P. peloponnesiacus* (Poulakakis et al., 2005b) and *L. trilineata* (Sagonas et al., 2014), the mammal *Talpa stankovici* (Tryfonopoulos et al., 2010), the land snails *Codringtonia* (Kotsakiozi et al., 2012) and *Josephinella* (Psonis et al., 2015), and the beetle *Gnaptor boryi* (Gkontas et al., 2016). Intense tectonic rearrangements during the Pliocene caused an important size reduction of the Peloponnese, with the present mountainous areas being the only non-submerged land surfaces (Creutzburg, 1963). Thus, only mountain foots and plateaus were able to host suitable habitats, while mountains acted as biogeographic barriers that prevented gene flow among populations.

### 4.6. Pleistocene climatic oscillations, eustatic changes, and glacial refugia

During the Pleistocene, the glacial and interglacial periods caused eustatic changes that greatly affected the intraspecific genetic diversity and relationships of insular and coastal *Podarcis* populations. *Podarcis gaigeae* displayed low genetic diversity, shallow and unresolved relationships among individuals, a star-like mtDNA haplotype network, weak population structure, as well as demographic equilibrium (according to mtDNA) or partial population expansion (according to microsatellites). These results suggest a recent genetic differentiation, which is in agreement with Runemark et al. (2012) and the recent paleogeography of the Skyros island group. Indeed, the present form consisting of a main island and several satellite islets, is the result of Lower Pleistocene geographic fragmentation due to eustatic changes caused by climatic oscillations (Perissoratis and Conispoliatis, 2003; van Andel and Shackleton, 1982). Similarly, the current distribution of *P. milensis*, although with higher nucleotide diversity than *P. gaigeae*, is the result of very recent eustatic-driven island isolations (Lambeck, 1996). Geographic fragmentation due to sea level changes has been considered as the most important factor of differentiation also in the case of the Cyclades populations of *P. erhardii* (Hurston et al., 2009).

The divergence among the three phylogenetic subclades of *P. melisellensis* was estimated at 1.2–1.9 Mya by Podnar et al. (2004), hypothesizing that a gradual sea level rise during the Pleistocene (De Giuli et al., 1987) caused the split among its three subclades. Finally, the differentiation of *P. tauricus* population of Thasopoula islet in North Aegean revealed by the microsatellites dataset, might be attributed to a founder event.

The distributional pattern of *P. ionicus* lineages is quite interesting. On one side, there is a group of lineages (subclade *e*) that are widely distributed in the Peloponnese (Fig. S10) and in western Greece, and on the other there is a group of lineages (the four other subclades) with a very restricted distribution, mainly in the Peloponnese (Figs. S11 and S12). The first group showed low genetic diversity, indicating recent expansion. The demographic analyses, such as the mtDNA BSP, the microsatellite k-test and BOTTLENECK, suggested a post-bottleneck sudden expansion in the recent past. This concurs with the SDM projections for LGM and LIG of *P. ionicus* in western Greece and Albania, showing a considerable reduction of the potential distribution during the glacial/interglacial cycle compared to the present. The higher genetic diversity of *P. ionicus* subclades in the Peloponnese compared to western Greece and Albania, indicates that the direction of the spatial expansion is more likely to have happened from the Peloponnese to the north, a pattern also proposed for isopods and land snails (Klossa-Kilia et al., 2006; Kotsakiozi et al., 2012; Parmakelis et al., 2008; Psonis et al., 2015).

The effect of the Pleistocene glacial-interglacial periods on the diversification of other Balkan amphibians and reptiles [i.e. *Anguis* (Jablonski et al., 2016), *Triturus* (Wielstra et al., 2013), *Vipera ursinii* (Zinenko et al., 2015), *L. viridis* (Marzahn et al., 2016), *P. muralis* (Salvi et al., 2013), *Dalmatolacerta oxycephala* and *Dinarolacerta mosorensis* (Podnar et al., 2014)] led to the discovery of several climatic refugia in the southern Balkans. These local refugia gave rise to the hypothesis of 'refugia within refugia', according to which geographic (habitat richness) and climatic heterogeneity within the major glacial refugia may have provided discrete regions where populations diverged (Abellán and Svenning, 2014; Gomez and Lunt, 2007). Based on the dispersal ability of a species and the opportunities for post-glacial expansion to the north, a lineage or species can be characterized either as a 'post-glacial re-colonizer', which is the main biogeographic pattern leading to 'southern richness - northern purity' (Hewitt, 2000; Hewitt, 1999), or as a 'refugial endemic' with limited expansion potential (Bilton et al., 1998; Kryštufek et al., 2007).

According to the present study, the focal *P. tauricus* species subgroup includes both of these types, with *P. tauricus* being a prime example of a post-glacial colonizer. The mtDNA phylogenetic relationships within this taxon are unresolved, forming a characteristic comb-like shape with short branch lengths. The wide distribution range of this taxon, combined with the demographic analyses results, suggest a recent post-bottleneck spatial expansion of *P. tauricus.* This expansion happened from south to north during interglacial periods or after the end of the LGM that possibly caused the bottleneck, and from east to west, as indicated by the k-test on microsatellites that showed population expansion only of the eastern populations (Crimean Peninsula, Moldavia, and Ukraine). The SDM projections for the LGM and the LIG underpinned this hypothesis by showing a considerable reduction of the potential distribution in most of the taxon's range, with only a few spots exhibiting increased probability of potential presence in the southern Balkans and Eastern Europe (Fig. S16X). The southern Balkans could be considered as a local climatic refugium (Joger et al., 2007; Taberlet et al., 1998), also suggested by other phylogeographic studies on Balkan Lacertidae (Marzahn et al., 2016; Sagonas et al., 2014). The Crimean Peninsula (Fig. 1A) and the surrounding area could also be considered as another local refugium, hosting a distinct genetic population, as indicated by the microsatellite data (Fig. 3B). During glacial maxima, the regression of the Black Sea exposed a wide shelf connecting Crimea with the Balkans. The revealed mtDNA haplotype diversity in the Crimean Peninsula suggests that this territory acted as a diversity 'pocket', receiving colonization waves from south Balkans to the northeastern Europe. In this framework, the subclade *e* of *P. ionicus* is probably another post-glacial colonizer, whereas the rest of *P. ionicus* subclades are examples of glacial endemics that are confined by geographical barriers (e.g., mountains, islands).

## 5. Conclusions

Here we provide evidence that the integration of different types of molecular markers and the utilization of multiple methods is crucial in uncovering detailed processes that shape the evolutionary history of species groups throughout space and time. Previously unresolved phylogenetic relationships that appeared as polytomies by analysis of

traditional sequence data, were here resolved using genome-wide data, obtained by ddRADseq. Moreover, by genotyping microsatellites for hundredths of samples from the entire distribution of the *P. tauricus* species group we confirmed the existence of at least two cryptic evolutionary lineages and we revealed extensive population structuring. Our proposed phylogeographic scenario of the *P. tauricus* species subgroup identifies the Messinian Salinity Crisis as the main event causing species divergence, and Pliocene tectonic events and Quaternary climatic oscillations as the main drivers of the observed intraspecific patterns of genetic diversity. The current high-throughput sequencing approaches have the potential to address previously intractable questions in evolution of non-model organisms (Carstens et al., 2012; Goodwin et al., 2016; Lemmon and Lemmon, 2013), leading to the development of large-scale sequencing arrays based on reduced genome representations, which may provide thousands of markers densely covering the genome data at moderate to low costs (such as ddRADseq). However, the main drawback of these approaches concerns the performance and efficiency of software available for estimating divergence times, to handle large datasets, such as those obtained by ddRADseq. Advance in this field is expected to provide more robust estimates and reduce uncertainty.

## Data accessibility

The datasets generated during this study are available (in PHILIP format) from the corresponding author upon request.

## Acknowledgements

We wish to express our gratitude to (in alphabetical order): Roman Alekseev, Miguel A. Carretero, Igor Doronin, Arkadyi Dovzhenko, Daniel Gruľa, Václav Gvoždík, Tomáš Husák, Daniel Koleska, Spartak Litvinchuk, Andrey Matvyeyev, Edvárd Mizsei, Anton Nadolnyi, Panayiotis Pafilis, Boyan Petrov, Georgi Popgeorgiev, Konstantinos Sagonas, Leonid Sokolov, Konstantinos Sotiropoulos, Ivan Stolárik, Ilias Strachinis, Manos Stratakis, Helen Sviridenko, Vladimir Tsurcanu, Nikolay Tzankov, and Judit Vörös, for sending us several tissue samples or for their assistance in the field. We also thank the Municipal Port Fund of Keramoti and the fishing boat 'Parmenides' for helping us traveling to Thasopoula islet (North Aegean), and to Apostolos Trichas (NHMC) for the lizard's photograph used in the graphical abstract. Finally, we express our gratitude to Adalgisa Caccone (Yale University) for her help and advice on ddRADseq libraries' preparation.

This study was part of the EcoGenoDiv project funded by NSFR 2007-2013 programme for development, European Social Fund, Operational Programme, Education and Lifelong Learning investing in knowledge society, Ministry of Education and Religious Affairs, Managing Authority, Co-financed by Greece and the European Union. JCI was funded by Grant No. 173025 Ministry of Education, Science and Technological Development of Republic of Serbia. DJ was supported by the Slovak Research and Development Agency under the contract no. APVV-15-0147. Part of this work was funded by the Klaus Tschira Foundation.

## Author Contributions

NP (Psonis) collected samples, performed laboratory work, analyzed data and wrote the manuscript. AA, EK, and PK performed laboratory work, analyzed the data and commented on the manuscript. DD, AK, AS, ADL advised on the phylogenetic analyses on ddRADseq data and commented on the manuscript. DP performed the SDM. OK, DJ, JCI, IG, PL collected or provided samples. NP (Poulakakis) designed and supervised the research and refined the manuscript. All authors read and improved the final manuscript.

## Conflict of interest

The authors have no conflict of interest to declare.

## Appendix A. Supplementary material

Supplementary data associated with this article can be found, in the online version, at https://doi.org/10.1016/j.ympev.2018.03.021.

## References

Abellán, P., Svenning, J., 2014. Refugia within refugia – patterns in endemism and genetic divergence are linked to Late Quaternary climate stability in the Iberian Peninsula. Biol. J. Linnean Soc. 113, 13–28.
Aberer, A.J., Kobert, K., Stamatakis, A., 2014. ExaBayes: Massively Parallel Bayesian Tree Inference for the Whole-Genome Era. Mol. Biol. Evol. 31, 2553–2556.
Ahmadzadeh, F., Flecks, M., Carretero, M.A., Böhme, W., Ihlow, F., Kapli, P., Miraldo, A., Rödder, D., 2016. Separate histories in both sides of the Mediterranean: phylogeny and niche evolution of ocellated lizards. J. Biogeogr.
Ahmadzadeh, F., Flecks, M., Rödder, D., Böhme, W., Ilgaz, Ç., Harris, D.J., Engler, J.O., Üzüm, N., Carretero, M.A., 2013. Multiple dispersal out of Anatolia: biogeography and evolution of oriental green lizards. Biol. J. Linnean Soc. 110, 398–408.
Akın, Ç., Can Bilgin, C., Beerli, P., Westaway, R., Ohst, T., Litvinchuk, S.N., Uzzell, T., Bilgin, M., Hotz, H., Guex, G.D., Plötner, J., 2010. Phylogeographic patterns of genetic diversity in eastern Mediterranean water frogs were determined by geological processes and climate change in the Late Cenozoic. J. Biogeography 37, 2111–2124.
Allegrucci, G., Rampini, M., Gratton, P., Todisco, V., Sbordoni, V., 2009. Testing phylogenetic hypotheses for reconstructing the evolutionary history of *Dolichopoda* cave crickets in the eastern Mediterranean. J. Biogeography 36, 1785–1797.
Amos, W., Hoffman, J.I., Frodsham, A., Zhang, L., Best, S., Hill, A.V.S., 2007. Automated binning of microsatellite alleles: problems and solutions. Mol. Ecol. Notes 7, 10–14.
Antoniou, A., Kasapidis, P., Kotoulas, G., Mylonas, C.C., Magoulas, A., 2017. Genetic diversity of Atlantic Bluefin tuna in the Mediterranean Sea: insights from genome-wide SNPs and microsatellites. J. Biol. Res. (Thessalon) 24, 3.
Araújo, M.B., Guisan, A., 2006. Five (or so) challenges for species distribution modelling. J. Biogeography 33, 1677–1688.
Barbosa, S., Paupério, J., Herman, J.S., Ferreira, C.M., Pita, R., Vale-Gonçalves, H.M., Cabral, J.A., Garrido-García, J.A., Soriguer, R.C., Beja, P., Mira, A., Alves, P.C., Searle, J.B., 2017. Endemic species may have complex histories: within-refugium phylogeography of an endangered Iberian vole. Mol. Ecol. Notes 26, 951–967.
Belkhir, K., Borsa, P., Chikhi, L., Raufaste, N., Bonhomme, F., 2001. GENETIX, logiciel sous Windows TM pour la génétique des populations. Laboratoire Génome, Populations, Interactions CNRS UMR 5000: Université de Montpellier II, Montpellier, France.
Bilgin, R., 2007. Kgtests: a simple Excel Macro program to detect signatures of population expansion using microsatellites. Mol. Ecol. Notes 7, 416–417.
Bilton, D.T., Mirol, P.M., Mascheretti, S., Fredga, K., Zima, J., Searle, J.B., 1998. Mediterranean Europe as an area of endemism for small mammals rather than a source for northwards postglacial colonization. Proc. Biol. Sci. 265, 1219–1226.
Blois, J.L., 2012. update: Recent advances in using species distributional models to understand past distributions. Front. Biogeogr. 3, 123–124.
Blondel, J., Aronson, J., 1999. Biology and Wildlife of the Mediterranean Region. Oxford University Press.
Blondel, J., Aronson, J., Bodiou, J.Y., 2010. The Mediterranean Region: Biological Diversity through Time and Space. Oxford University Press.
Bouckaert, R.R., Heled, J., Kühnert, D., Vaughan, T.J., Wu, C., Xie, D., Suchard, M.A., Rambaut, A., Drummond, A.J., 2014. BEAST 2: A Software Platform for Bayesian Evolutionary Analysis. PLoS Comput. Biol. 10, e1003537.
Brown, R.P., Terrasa, B., Pırez-Mellado, V., Castro, J.A., Hoskisson, P.A., Picornell, A., Ramon, M.M., 2008. Bayesian estimation of post-Messinian divergence times in Balearic Island lizards. Mol. Phylogenet. Evol. 48, 350–358.
Bruford, M.W., Hanotte, O., Burke, T., 1998. Multi and single locus DNA fingerprinting. In: Hoelzel, A.R. (Ed.), Molecular Genetic Analysis of Populations: A Practical Approach. IRL Press, pp. 225–269.
Carstens, B.C., Lemmon, A.R., Lemmon, E.M., 2012. The promises and pitfalls of next-generation sequencing data in phylogeography. Syst. Biol. 61, 713–715.
Čerňanský, A., 2010. Earliest world record of green lizards (Lacertilia, Lacertidae) from the Lower Miocene of Central Europe. Biologia 65, 737–741.
Chifman, J., Kubatko, L.S., 2014. Quartet inference from SNP data under the coalescent model. Bioinformatics 30, 3317–3324.
Cornuet, J.M., Luikart, G., 1996. Description and power analysis of two tests for detecting recent population bottlenecks from allele frequency data. Genetics 144, 2001–2014.
Cox, S.C., Carranza, S., Brown, R.P., 2010. Divergence times and colonization of the Canary Islands by *Gallotia* lizards. Mol. Phylogenet. Evol. 56, 747–757.
Creutzburg, N., 1963. Paleogeographic evolution of Crete from Miocene till our days. Cretan Annals 15 (16), 336–342.
Crowley, T.J., North, G.R., 1991. Paleoclimatology. Oxford University Press, New York.
DaCosta, J.M., Sorenson, M.D., 2016. ddRAD-seq phylogenetics based on nucleotide, indel, and presence–absence polymorphisms: analyses of two avian genera with contrasting histories. Mol. Phylogenet. Evol. 94 (Part A), 122–135.
Darriba, D., Taboada, G.L., Doallo, R., Posada, D., 2012. jModelTest 2: more models, new heuristics and parallel computing. Nat. Meth. 9 772-772.

De Giuli, C., Masini, F., Valleri, G., 1987. Paleogeographic evolution of the Adriatic area since Oligocene to Pleistocene. Riv. It. Paleont. Strat. 93, 109–126.
Dermitzakis, D.M., 1989. The colonisation of Aegean islands in relation with the paleogeographic evolution (in greek). Biol. Gallo-Hellenica 14, 99–121.
Dermitzakis, D.M., 1990. Paleogeography, Geodynamic Processes and event Stratigraphy during the Late Cenozoic of the Aegean area. Atti Convegni Lincei 85, 263–288.
Dermitzakis, D.M., Papanikolaou, D.J., 1981. Paleogeography and geodynamics of the Aegean region during the Neogene. Annal. Geol. Pays Hellenic 30, 245–289.
Džukić, G., Kalezić, M.L., 2004. The Biodiversity of Amphibians and Reptiles in the Balkan Peninsula. In: Griffiths, H.I. (Ed.), Balkan Biodiversity: Pattern and Process in the European Hotspot. Kluwer Academic Publishers, Dordrecht, pp. 167–792.
Earl, D.A., vonHoldt, B.M., 2012. STRUCTURE HARVESTER: a website and program for visualizing STRUCTURE output and implementing the Evanno method. Conserv. Genet. Res. 4, 359–361.
Eaton, D.A.R., 2014. PyRAD: assembly of de novo RADseq loci for phylogenetic analyses. Bioinformatics 30, 1844–1848.
Estes, R., 1983. Handbuch der Paläoherpetologie, Part 10: Sauria terrestria. Gustav Fischer Verlag, Stuttgart, Amphisbaenia.
Evanno, G., Regnaut, S., Goudet, J., 2005. Detecting the number of clusters of individuals using the software STRUCTURE: a simulation study. Mol Ecol 14, 2611–2620.
Ferchaud, A., Ursenbacher, S., Cheylan, M., Luiselli, L., Jelić, D., Halpern, B., Major, Á., Kotenko, T., Keyan, N., Behrooz, R., Crnobrnja-Isailović, J., Tomović, L., Ghira, I., Ioannidis, Y., Arnal, V., Montgelard, C., 2012. Phylogeography of the *Vipera ursinii* complex (Viperidae): mitochondrial markers reveal an east–west disjunction in the Palaearctic region. J. Biogeogr. 39, 1836–1847.
Gariboldi, M.C., Túnez, J.I., Failla, M., Hevia, M., Panebianco, M.V., Paso Viola, M.N., Vitullo, A.D., Cappozzo, H.L., 2016. Patterns of population structure at microsatellite and mitochondrial DNA markers in the franciscana dolphin (*Pontoporia blainvillei*). Ecol. Evol. 6, 8764–8776.
Gkontas, I., Papadaki, S., Trichas, A., Poulakakis, N., 2016. First assessment on the molecular phylogeny and phylogeography of the species *Gnaptor boryi* distributed in Greece (Coleoptera: Tenebrionidae). Mitoch. DNA Part A 1–8.
Gomez, A., Lunt, D.H., 2007. Refugia within refugia: patterns of phylogeographic concordance in the Iberian Peninsula. In: Weiss, S., Ferrand, N. (Eds.), Phylogeography in Southern European Refugia: Evolutionary Perspectives On the Origins and Conservation of European Biodiversity. Springer, Berlin, pp. 155–188.
Goodwin, S., McPherson, J.D., McCombie, W.R., 2016. Coming of age: ten years of next-generation sequencing technologies. Nat. Rev. Gen. 17, 333.
Griffiths, H., Kryštufek, B., Reed, J., 2004. Balkan Biodiversity: Pattern and Process in the European Hotspot. Springer.
Guicking, D., Joger, U., Wink, M., 2009. Cryptic diversity in a Eurasian water snake (*Natrix tessellata*, Serpentes: Colubridae): evidence from mitochondrial sequence data and nuclear ISSR-PCR fingerprinting. Org. Divers. Evol. 9, 201–214.
Guillou, H., Carracedo, J.C., Torrado, F.P., Badiola, E.R., 1996. K-Ar ages and magnetic stratigraphy of a hotspot-induced, fast grown oceanic island: El Hierro, Canary Islands. J. Volcanol. Geoth. Res. 73, 141–155.
Gvoždík, V., Jandzik, D., Lymberakis, P., Jablonski, D., Moravec, J., 2010. Slow worm, *Anguis fragilis* (Reptilia: Anguidae) as a species complex: genetic structure reveals deep divergences. Mol. Phylogenet. Evol. 55, 460–472.
Harris, J.D., Arnold, N.E., 1999. Relationships of wall lizards, *Podarcis* (Reptilia: Lacertidae) based on mitochondrial DNA sequences. Copeia 749–754.
Hewitt, G., 2000. The genetic legacy of the Quaternary ice ages. Nature 405, 907–913.
Hewitt, G.M., 1999. Post-glacial re-colonization of European biota. Biol. J. Linnean Soc. 68, 87–112.
Hewitt, G.M., 2011. Mediterranean Peninsulas: The Evolution of Hotspots. Springer Publishers, Berlin Heidelberg, Biodiversity Hotspots.
Hijmans, R.J., Cameron, S.E., Parra, J.L., Jones, P.G., Jarvis, A., 2005. Very high resolution interpolated climate surfaces for global land areas. Int. J. Climatol. 25, 1965–1978.
Hsü, K.J., 1972. Origin of saline giants: a critical review after the discovery of the Mediterranean Evaporite. Earth-Science Rev. 8, 371–396.
Hurston, H., Voith, L., Bonanno, J., Foufopoulos, J., Pafilis, P., Valakos, E., Anthony, N., 2009. Effects of fragmentation on genetic diversity in island populations of the Aegean wall lizard *Podarcis erhardii* (Lacertidae, Reptilia). Mol. Phylogenet. Evol. 52, 395–405.
Jablonski, D., Jandzik, D., Mikulíček, P., Džukić, G., Ljubisavljević, K., Tzankov, N., Jelić, D., Thanou, E., Moravec, J., Gvoždík, V., 2016. Contrasting evolutionary histories of the legless lizards slow worms (*Anguis*) shaped by the topography of the Balkan Peninsula. BMC Evol. Biol. 16, 1–18.
Jakobsson, M., Rosenberg, N.A., 2007. CLUMPP: a cluster matching and permutation program for dealing with label switching and multimodality in analysis of population structure. Bioinformatics 23, 1801–1806.
Joger, U., Fritz, U., Guicking, D., Kalyabina-Hauf, S., Nagy, Z.T., Wink, M., 2007. Phylogeography of western Palaearctic reptiles – spatial and temporal speciation patterns. Zool. Anz. 246, 293–313.
Jolivet, L., Augier, R., Robin, C., Suc, J., Rouchy, J., 2006. Lithospheric-scale geodynamic context of the Messinian salinity crisis. Sediment. Geol. 188–189, 9–33.
Jombart, T., Ahmed, I., 2011. adegenet 1.3-1: new tools for the analysis of genome-wide SNP data. Bioinformatics.
Jombart, T., Devillard, S., Balloux, F., 2010. Discriminant analysis of principal components: a new method for the analysis of genetically structured populations. BMC Genetics 11, 1–15.
Kalinowski, S.T., Wagner, A.P., Taper, M.L., 2006. ml-relate: a computer program for maximum likelihood estimation of relatedness and relationship. Mol. Ecol. Notes 6, 576–579.
Kaliontzopoulou, A., Brito, J.C., Carretero, M.A., Larbes, S., Harris, D.J., 2008. Modelling the partially unknown distribution of wall lizards (*Podarcis*) in North Africa: ecological affinities, potential areas of occurrence, and methodological constraints. Canadian J. Zool. 86, 992–1001.
Katoh, K., Standley, D.M., 2013. MAFFT Multiple Sequence Alignment Software Version 7: Improvements in Performance and Usability. Mol. Biol. Evol. 30, 772–780.
Kenneth, J.H., Montadert, L., Bernoulli, D., Cita, M.B., Erickson, A., Garrison, R.E., Kidd, R.B., Melieres, F., Muller, C., Wright, R.A., 1977. History of the Mediterranean salinity crisis. Nature 267, 399–403.
Kindler, C., Böhme, W., Corti, C., Gvoždík, V., Jablonski, D., Jandzik, D., Metallinou, M., Široký, P., Fritz, U., 2013. Mitochondrial phylogeography, contact zones and taxonomy of grass snakes (*Natrix natrix*, *N. megalocephala*). Zool. Scripta 42, 458–472.
King, J.P., Kimmel, M., Chakraborty, R., 2000. A power analysis of microsatellite-based statistics for inferring past population growth. Mol. Biol. Evol. 17, 1859–1868.
Klossa-Kilia, E., Kilias, G., Tryfonopoulos, G., Koukou, K., Spyros, S., Parmakelis, A., 2006. Molecular phylogeny of the Greek populations of the genus *Ligidium* (Isopoda, Oniscidea) using three mtDNA gene segments. Zool. Scr. 35, 459–472.
Kornilios, P., Thanou, E., Kapli, P., Parmakelis, A., Chatzaki, M., 2016. Peeking through the trapdoor: historical biogeography of the Aegean endemic spider Cyrtocarenum Ausserer, 1871 with an estimation of mtDNA substitution rates for Mygalomorphae. Mol. Phylogenet. Evol.
Kotsakiozi, P., Parmakelis, A., Giokas, S., Papanikolaou, I., Valakos, E.D., 2012. Mitochondrial phylogeny and biogeographic history of the Greek endemic land-snail genus *Codringtonia* Kobelt 1898 (Gastropoda, Pulmonata, Helicidae). Mol. Phylogenet. Evol. 62, 681–692.
Kozlov, A.M., Aberer, A.J., Stamatakis, A., 2015. ExaML Version 3: A Tool for Phylogenomic Analyses on Supercomputers. Bioinformatics.
Krijgsman, W., Hilgen, F.J., Raffi, I., Sierro, F.J., Wilson, D.S., 1999. Chronology, causes and progression of the Messinian salinity crisis. Nature 400, 652–655.
Kryštufek, B., Buzan, E.V., Hutchinson, W.F., Hänfling, B., 2007. Phylogeography of the rare Balkan endemic Martino's vole, *Dinaromys bogdanovi*, reveals strong differentiation within the western Balkan Peninsula. Mol. Ecol. 16, 1221–1232.
Kuhlemann, J., 2007. Paleogeographic and paleotopographic evolution of the Swiss and Eastern Alps since the Oligocene. Glob. Planet. Change 58, 224–236.
Lambeck, K., 1996. Sea-level change and shore-line evolution in Aegean Greece since upper palaeolithic time. Antiquity 70, 588–611.
Leaché, A.D., Chavez, A.S., Jones, L.N., Grummer, J.A., Gottscho, A.D., Linkem, C.W., 2015. Phylogenomics of phrynosomatid lizards: conflicting signals from sequence capture versus restriction site associated DNA sequencing. Genome Biol. Evol. 7, 706–719.
Lemmon, E.M., Lemmon, A.R., 2013. High-throughput genomic data in systematics and phylogenetics. Annu. Rev. Ecol. Evol. Syst. 44, 99–121.
Lymberakis, P., Poulakakis, N., 2010. Three continents claiming an archipelago: the evolution of Aegean's herpetofaunal diversity. Diversity 2, 233–255.
Lymberakis, P., Poulakakis, N., Manthalou, G., Tsigenopoulos, C.S., Magoulas, A., Mylonas, M., 2007. Mitochondrial phylogeography of *Rana (Pelophylax)* populations in the Eastern Mediterranean region. Mol. Phylogenet. Evol. 44, 115–125.
Marzahn, E., Mayer, W., Joger, U., Ilgaz, Ç., Jablonski, D., Kindler, C., Kumlutaş, Y., Nistri, A., Schneeweiss, N., Vamberger, M., Žagar, A., Fritz, U., 2016. Phylogeography of the *Lacerta viridis* complex: mitochondrial and nuclear markers provide taxonomic insights. J. Zool. Syst. Evol. Res. 54, 85–105.
Mayer, W., Beyerlein, P., 2001. Genetic differentiation of the *Lacerta viridis/bilineata* complex and of *Lacerta trilineata* in Greece: mitochondrial DNA sequences. Mertensiella 13, 52–59.
Meulenkamp, J.E., 1985. Aspects of the Late Cenozoic Evolution of the Aegean Region. In: Stanley, D.J., Wezel, F.C. (Eds.), Geological Evolution of the Mediterranean Basin. Springer, New York, pp. 307–321.
Mizsei, E., Jablonski, D., Roussos, S.A., Dimaki, M., Ioannidis, Y., Nilson, G., Nagy, Z.T., 2017. Nuclear markers support the mitochondrial phylogeny of Vipera ursinii-renardi complex (Squamata: Viperidae) and species status for the Greek meadow viper. Zootaxa 4227, zootaxa.4227.4221.4224.
Musilová, R., Zavadil, V., Marková, S., Kotlík, P., 2010. Relics of the Europe's warm past: phylogeography of the Aesculapian snake. Mol. Phylogenet. Evol. 57, 1245–1252.
Myers, N., Mittermeier, R.A., Mittermeier, C.G., da Fonseca, G.A.B., Kent, J., 2000. Biodiversity hotspots for conservation priorities. Nature 403, 853–858.
Nei, M., 1987. Molecular Evolutionary Genetics. Columbia University Press, New York.
Nieto-Montes de Oca, A., Barley, A.J., Meza-Lázaro, R.N., García-Vázquez, U.O., Zamora-Abrego, J.G., Thomson, R.C., Leaché, A.D., 2017. Phylogenomics and species delimitation in the knob-scaled lizards of the genus *Xenosaurus* (Squamata: Xenosauridae) using ddRADseq data reveal a substantial underestimation of diversity. Mol. Phylogenet. Evol. 106, 241–253.
Ogilvie, H.A., Bouckaert, R.R., Drummond, A.J., 2017. StarBEAST2 brings faster species tree inference and accurate estimates of substitution rates. Mol. Biol. Evol.
Oliverio, M., Bologna, M.A., Mariottini, P., 2000. Molecular biogeography of the Mediterranean lizards *Podarcis* Wagler, 1830 and *Teira* Gray, 1838 (Reptilia, Lacertidae). J. Biogeography 27, 1403–1420.
Parmakelis, A., Klossa-Kilia, E., Kilias, G., Triantis, K.A., Sfenthourakis, S., 2008. Increased molecular divergence of two endemic *Trachelipus* (Isopoda, Oniscidea) species from Greece reveals patterns not congruent with current taxonomy. Biol. J. Linnean Soc. 95, 361–370.
Pattengale, N.D., Alipour, M., Bininda-Emonds, O.R., Moret, B.M., Stamatakis, A., 2010. How many bootstrap replicates are necessary? J. Comput. Biol.: J. Comput. Mol. Cell Biol. 17, 337–354.
Pavlicev, M., Mayer, W., 2009. Fast radiation of the subfamily Lacertinae (Reptilia: Lacertidae): History or methodical artefact? Mol. Phylogenet. Evol. 52, 727–734.
Perissoratis, C., Conispoliatis, N., 2003. The impacts of sea-level changes during latest Pleistocene and Holocene times on the morphology of the Ionian and Aegean seas (SE

Alpine Europe). Mar. Geol. 196, 145–156.
Peterson, B.K., Weber, J.N., Kay, E.H., Fisher, H.S., Hoekstra, H.E., 2012. Double digest RADseq: an inexpensive method for *De Novo* SNP discovery and genotyping in model and non-model species. PLoS ONE 7, e37135.
Phillips, J.S., Dudik, M., Schapire, E.R., 2004. A maximum entropy approach to species distribution modeling. In: Proc. 21st ICML. ACM, Banff, Alberta, Canada, p. 83.
Phillips, S.J., Anderson, R.P., Schapire, R.E., 2006. Maximum entropy modeling of species geographic distributions. Ecol. Model 190, 231–259.
Piry, S., Luikart, G., Cornuet, J.M., 1999. BOTTLENECK: a computer program for detecting recent reductions in the effective population size using allele frequency data. J. Heredity 90, 502–503.
Podnar, M., Madaric, B.B., Mayer, W., 2014. Non concordant phylogeographical patterns of three widely codistributed endemic Western Balkans lacertid lizards (Reptilia, Lacertidae) shaped by specific habitat requirements and different responses to Pleistocene climatic oscillations. J. Zool. Syst. Evol. Res. 52, 119–129.
Podnar, M., Mayer, W., Tvrtković, N., 2004. Mitochondrial phylogeography of the Dalmatian wall lizard, (Lacertidae). Org. Divers. Evol. 4, 307–317.
Popov, S.V., Rögl, F., Rozanov, A.Y., Steininger, F.F., Shcherba, I.G., Kovac, M., 2004. Lithological-Paleogeographic Maps of Paratethys. Schweizerbart'sche Verlagsbuchhandlung.
Potts, R., Behrensmeyer, A.K., 1992. Late Cenozoic terrestrial ecosystems. In: Behrensmeyer, A.K., Damuth, J., DiMichele, W., Potts, R., Sues, H.D., Wing, S. (Eds.), Terrestrial Ecosystems through Time. University of Chicago Press, Chicago, pp. 419–541.
Poulakakis, N., Kapli, P., Lymberakis, P., Trichas, A., Vardinoyannis, K., Sfenthourakis, S., Mylonas, M., 2014. A review of phylogeographic analyses of animal taxa from the Aegean and surrounding regions. J. Zool. Syst. Evol. Res. 53, 18–32.
Poulakakis, N., Lymberakis, P., Valakos, E., Pafilis, P., Zouros, E., Mylonas, M., 2005a. Phylogeography of Balkan wall lizard (*Podarcis taurica*) and its relatives inferred from mitochondrial DNA sequences. Mol Ecol 14, 2433–2443.
Poulakakis, N., Lymberakis, P., Valakos, E., Zouros, E., Mylonas, M., 2005b. Phylogenetic relationships and biogeography of *Podarcis* species from the Balkan Peninsula, by bayesian and maximum likelihood analyses of mitochondrial DNA sequences. Mol. Phylogenet. Evol. 37, 845–857.
Pritchard, J.K., Stephens, M., Donnelly, P., 2000. Inference of population structure using multilocus genotype data. Genetics 155, 945–959.
Psonis, N., Antoniou, A., Kukushkin, O., Jablonski, D., Petrov, B., Crnobrnja-Isailović, J., Sotiropoulos, K., Gherghel, I., Lymberakis, P., Poulakakis, N., 2017. Hidden diversity in the *Podarcis tauricus* (Sauria, Lacertidae) species subgroup in the light of multilocus phylogeny and species delimitation. Mol. Phylogenet. Evol. 106, 6–17.
Psonis, N., Lymberakis, P., Poursanidis, D., Poulakakis, N., 2016. Contribution to the study of *Acanthodactylus* (Sauria: Lacertidae) mtDNA diversity focusing on the *A. boskianus* species group. Mitochondrion 30, 78–94.
Psonis, N., Vardinoyannis, K., Mylonas, M., Poulakakis, N., 2015. Unraveling the evolutionary history of the *Chilostoma* Fitzinger, 1833 (Mollusca, Gastropoda, Pulmonata) lineages in Greece. Mol. Phylogenet. Evol. 91, 210–225.
Rato, C., Harris, D.J., Perera, A., Carvalho, S.B., Carretero, M.A., Rödder, D., 2015. A Combination of Divergence and Conservatism in the Niche Evolution of the Moorish Gecko, *Tarentola mauritanica* (Gekkota: Phyllodactylidae). PLoS ONE 10, e0127980.
Raymond, M., Rousset, F., 1995. Genepop (Version-1.2) - population-genetics software for exact tests and ecumenicism. J. Heredity 86, 248–249.
Ree, R.H., Smith, S.A., 2008. Maximum likelihood inference of geographic range evolution by dispersal, local extinction, and cladogenesis. Syst. Biol. 57, 4–14.
Reich, D.E., Feldman, M.W., Goldstein, D.B., 1999. Statistical properties of two tests that use multilocus data sets to detect population expansions. Mol. Biol. Evol. 16, 453–466.
Robinson, D.F., Foulds, L.R., 1981. Comparison of phylogenetic trees. Math. Biosci. 53, 131–147.
Rosenberg, N.A., 2004. distruct: a program for the graphical display of population structure. Mol. Ecol. Notes 4, 137–138.
Runemark, A., Hey, J., Hansson, B., Svensson, E.I., 2012. Vicariance divergence and gene flow among islet populations of an endemic lizard. Mol. Ecol. 21, 117–129.
Sagonas, K., Poulakakis, N., Lymberakis, P., Parmakelis, A., Pafilis, P., Valakos, E.D., 2014. Molecular systematics and historical biogeography of the green lizards (*Lacerta*) in Greece: insights from mitochondrial and nuclear DNA. Mol. Phylogenet. Evol. 76C, 144–154.
Salvi, D., Harris, D.J., Kaliontzopoulou, A., Carretero, M.A., Pinho, C., 2013. Persistence across Pleistocene ice ages in Mediterranean and extra-Mediterranean refugia: phylogeographic insights from the common wall lizard. BMC Evol. Biol. 13, 147.
Schoener, T.W., 1968. The *Anolis* Lizards of Bimini: resource partitioning in a complex Fauna. Ecology 49, 704–726.
Schule, W., 1993. Mammals, vegetation and the initial human settlement of the Mediterranean islands: a palaeoecological approach. J. Biogeography 20, 399–412.
Senczuk, G., Colangelo, P., De Simone, E., Aloise, G., Castiglia, R., 2017. A combination of long term fragmentation and glacial persistence drove the evolutionary history of the Italian wall lizard *Podarcis siculus*. BMC Evol. Biol. 17, 6.
Shriver, M.D., Jin, L., Chakraborty, R., Boerwinkle, E., 1993. VNTR allele frequency distributions under the stepwise mutation model: a computer simulation approach. Genetics 134, 983–993.
Sillero, N., Campos, J., Bonardi, A., Corti, C., Creemers, R., Crochet, P., Crnobrnja-Isailović, J., Denoël, M., Ficetola, G.F., Gonçalves, J., Kuzmin, S., Lymberakis, P., de Pous, P., Rodríguez, A., Sindaco, R., Speybroeck, J., Toxopeus, B., Vieites, D.R., Vences, M., 2014. Updated distribution and biogeography of amphibians and reptiles of Europe. Amphibia-Reptilia 35, 1–31.
Skourtanioti, E., Kapli, P., Ilgaz, Ç., Kumlutaş, Y., Avcı, A., Ahmadzadeh, F., Crnobrnja-Isailović, J., Gherghel, I., Lymberakis, P., Poulakakis, N., 2016. A reinvestigation of phylogeny and divergence times of the *Ablepharus kitaibelii* species complex (Sauria, Scincidae) based on mtDNA and nuDNA genes. Mol. Phylogenet. Evol. 103, 199–214.
Stamatakis, A., 2014. RAxML Version 8: a tool for phylogenetic analysis and post-analysis of large phylogenies. Bioinformatics 30, 1312–1313.
Steininger, F.F., Rögl, F., 1984. Paleogeography and palinspastic reconstruction of the Neogene of the Mediterranean and Paratethys. In: Dixon, J.E., Robertson, A.H.F. (Eds.), The Geological Evolution of the Eastern Meidterranean. Blackwell Scientific Publications, pp. 659–668.
Svenning, J., Fløjgaard, C., Marske, K.A., Nógues-Bravo, D., Normand, S., 2011. Applications of species distribution modeling to paleobiology. Quat. Sci. Rev. 30, 2930–2947.
Swofford, D.L., 2002. PAUP*. Phylogenetic analysis using parsimony (*and other methods). Version 4. Sinauer Associates, Sunderland, MA.
Taberlet, P., Fumagalli, L., Wust-Saucy, A.G., Cosson, J.F., 1998. Comparative phylogeography and postglacial colonization routes in Europe. Mol. Ecol. 7, 453–464.
Terrasa, B., Picornell, A., Castro, J.A., Ramon, M.M., 2004. Genetic variation within endemic *Podarcis* lizards from the Balearic Islands inferred from partial Cytochrome b sequences. Amphibia-Reptilia 25, 407–414.
Toonen, R.J., Hughes, S., 2001. Increased throughput for fragment analysis on an ABI PRISM 377 automated sequencer using a membrane comb and STRand software. Biotechniques 31, 1320–1324.
Tryfonopoulos, G., Thanou, E., Fraguedakis-Tsolis, S., Chondropoulos, B., 2010. New data on the distribution and genetic structure of Greek moles of the genus *Talpa* (Mammalia, Talpidae). J. Zool. Syst. Evol. Res. 48, 188–193.
Ursenbacher, S., Schweiger, S., Tomovic, L., Crnobrnja-Isailovic, J., Fumagalli, L., Mayer, W., 2008. Molecular phylogeography of the nose-horned viper (*Vipera ammodytes*, Linnaeus (1758)): evidence for high genetic diversity and multiple refugia in the Balkan peninsula. Mol. Phylogenet. Evol. 46, 1116–1128.
Vähä, J., Erkinaro, J., NiemelÄ, E., Primmer, C.R., 2007. Life-history and habitat features influence the within-river genetic structure of Atlantic salmon. Mol. Ecol. 16, 2638–2654.
Valakos, E., Pafilis, P., Sotiropoulos, K., Lymberakis, P., Maragou, P., Foufopoulos, J., 2008. The Amphibians and Reptiles of Greece. Chimaira, Frankfurt am Main.
van Andel, T.H., Shackleton, J.C., 1982. Late Paleolithic and Mesolithic Coastlines of Greece and the Aegean. J. Field Archaeology 9, 445–454.
van der Vaart, A.W., 1998. Asymptotic statistics. Cambridge University Press, Cambridge.
van Oosterhout, C., Hutchinson, W.F., Wills, D.P.M., Shipley, P., 2004. MICRO-CHECKER: software for identifying and correcting genotyping errors in microsatellite data. Mol. Ecol. Notes 4, 535–538.
Venczel, M., 2006. Lizards from the late Miocene of Polgárdi (W-Hungary). Nymphaea 33.
Warren, D.L., Glor, R.E., Turelli, M., 2008. Environmental niche equivalency versus conservatism: quantitative approaches to niche ecolution. Evolution 62, 2868–2883.
Warren, D.L., Glor, R.E., Turelli, M., 2010. ENMTools: a toolbox for comparative studies of environmental niche models. Ecography 33, 607–611.
Weir, B.S., Cockerham, C.C., 1984. Estimating F-statistics for the analysis of population-structure. Evolution 38, 1358–1370.
Welter-Schultes, F., 2012. European Non-Marine Molluscs, A Guide for Species Identification. Planet Poster Editions, Göttingen.
Wielstra, B., Crnobrnja-Isailovic, J., Litvinchuk, S., Reijnen, B., Skidmore, A., Sotiropoulos, K., Toxopeus, A., Tzankov, N., Vukov, T., Arntzen, J.W., 2013. Tracing glacial refugia of *Triturus* newts based on mitochondrial DNA phylogeography and species distribution modeling. Front. Zool. 10, 13.
Wilson, G.A., Rannala, B., 2003. Bayesian inference of recent migration rates using multilocus genotypes. Genetics 163, 1177–1191.
Yu, Y., Harris, A.J., He, X., 2013. RASP (Reconstruct Ancestral State in Phylogenies) 2.1 beta. Available at http://mnh.scu.edu.cn/soft/blog/RASP.
Zachos, J., Pagani, M., Sloan, L., Thomas, E., Billups, K., 2001. Trends, rhythms, and aberrations in global climate 65 Ma to present. Science 292, 686–693.
Zelilidis, A., Kontopoulos, N., Avramidis, P., Piper, D.J.W., 1998. Tectonic and sedimentological evolution of the Pliocene-Quaternary basins of Zakynthos island, Greece: case study of the transition from compressional to extensional tectonics. Basin Res. 10, 393–408.
Zinenko, O., Stümpel, N., Mazanaeva, L., Bakiev, A., Shiryaev, K., Pavlov, A., Kotenko, T., Kukushkin, O., Chikin, Y., Duisebayeva, T., Nilson, G., Orlov, N.L., Tuniyev, S., Ananjeva, N.B., Murphy, R.W., Joger, U., 2015. Mitochondrial phylogeny shows multiple independent ecological transitions and northern dispersion despite of Pleistocene glaciations in meadow and steppe vipers (*Vipera ursinii* and *Vipera renardi*). Mol. Phylogenet. Evol. 84, 85–100.